CONTRACT NAS 3-14348

IGNITION SYSTEM FOR SPACE SHUTTLE AUXILIARY PROPULSION SYSTEM

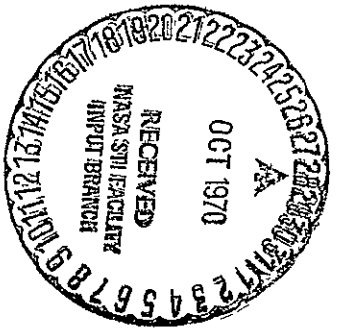

QUARTERLY TECHNICAL PROGRESS NARRATIVE 1678-26-Q-1

29 June-27 September 1970

Engine Components Department
Aerojet Liquid Rocket Company
Sacramento, California 95813

S. D. Rosenberg

17 October 1970

Prepared for NASA-Lewis Research Center
Cleveland, Ohio 44135

FOREWORD

Contract NAS 3-14348, "Ignition System for Space Shuttle Auxiliary Propulsion System," is being performed by the Aerojet Liquid Rocket Company at Sacramento, California. The performance period covered by this Quarterly Technical Progress Narrative is from 29 June through 27 September 1970.

The Program Manager is Dr. R. J. LaBotz, The Project Manager is Dr. S. D. Rosenberg. The Project Engineer is A. J. Aitken. The NASA Project Manager is E. A. Edelman, NASA-Lewis Research Center.

Approved:

R. J. LaBotz, Manager
APS Engine Programs
Engine Components Department

ABSTRACT

A Design Review of the spark and plasma pulse igniters for the high and low chamber pressure design points and the injectors and chambers associated therewith was held at ALRC on September 5 & 6, 1970. All design changes which resulted from this review were completed. Fabrication of the high P_c spark and plasma pulse igniters was completed. Fabrication of the companion igniters for the low P_c design point was initiated and is nearing completion.

Analytical work included heat transfer, stress and materials analysis in support of igniter design and the checkout and modification of the Transient Flow and Turbulent Mixing and Combustion Computer Programs.

Electrode Durability Tests with the spark igniter were completed satisfactorily. Nickel proved to be the best of the candidate materials, successfully surviving 10^6 spark discharges.

The setup of the facilities required for the conduct of the Igniter-Only Tests, Igniter-Complete Thruster Tests and Ignition Durability Tests was initiated.

TABLE OF CONTENTS

FIGURE LIST

TABLE OF CONTENTS (cont.)

FIGURE LIST (cont.)

TABLE LIST

I. INTRODUCTION

The objectives of this program are to obtain basic ignition data on spark and plasma torch ignition methods at operating conditions typical of the Space Shuttle Auxiliary Propulsion System and to complete a preliminary design of an optimum ignition system based upon the test results. The planned work will be comprised of: An analytical and experimental program of design, fabrication and testing of gaseous hydrogen-gaseous oxygen ignition systems with data obtained for wide ranges of operating conditions; and the completion of a preliminary design of a complete Space Shuttle Auxiliary Propulsion System ignition system.

A four task program is planned to achieve the program objectives: Task I - Igniter Design and Fabrication; Task II - Igniter Tests; Task III - Ignition System Preliminary Design; and Task IV - Reporting Requirements.

II. TECHNICAL PROGRESS

A. TASK I - IGNITER DESIGN AND FABRICATION

1. Design

a. Igniter Description

An isometric cutaway view of the high P_c spark igniter assembly is shown in Figure 1. This igniter is designed to operate in a dual mode, either as an ignition source for the APS engine or as a minimum impulse thruster. For this reason, the igniter is equipped with a separate set of propellant valves. This basic design has been proven to have a very fast response with a reproducible ignition delay on the order of 2 msec from the start of flow.

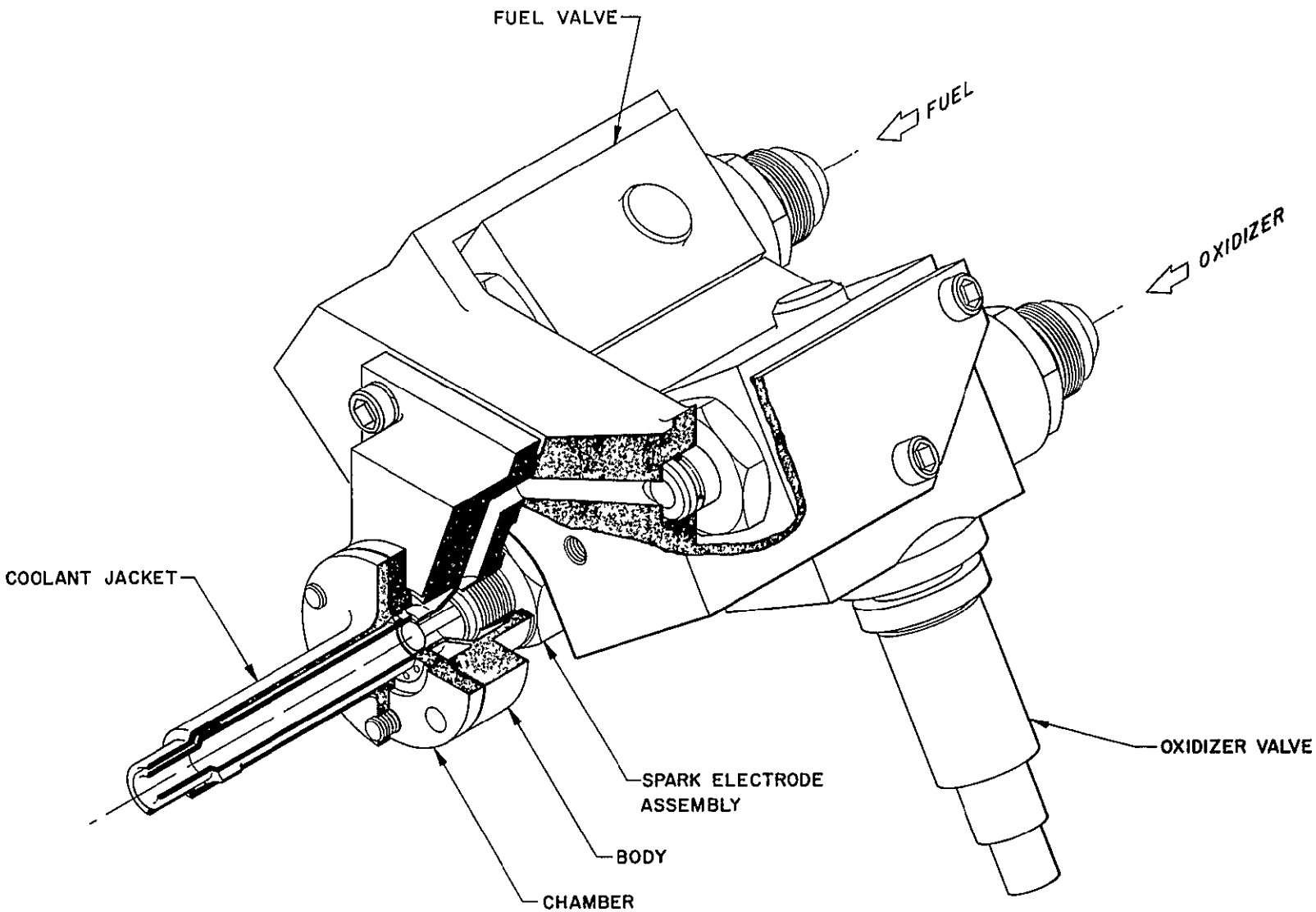

Figure 1. Oxygen/Hydrogen Spark Igniter Assembly

II, A, Task I - Igniter Design and Fabrication (cont.)

The basic igniter can be operated either with a spark discharge or with a plasma pulse discharge by replacing the spark electrode assembly with a plasma pulse assembly. In the configuration shown, the fuel and oxidizer are started simultaneously through the valve with the spark electrode energized.

The oxidizer flows from the oxidizer manifold around the spark electrode into the igniter chamber. This electrode arrangement provides cooling of the electrode which prevents erosion due to combustion gases. No electrode erosion has been experienced with this arrangement in over 1000 ignition tests.

The fuel flows from an annular manifold through parallel coolant and injector flow passages. A small portion of the hydrogen is injected into the igniter chamber where it impinges with the oxidizer flow just downstream of the spark electrode. The bulk of the hydrogen flow is ducted along the chamber backside wall for cooling during steady state operation.

In the plasma pulse configuration, the spark electrode assembly is replaced with a plasma pulse assembly and the valve adapter body is modified to allow hydrogen to be ducted to the plasma electrode. In this configuration, the hydrogen that is injected to combine with the oxygen in the spark mode, i.e., the core hydrogen, is now injected from the center of the plasma plug. The hydrogen coolant flow is identical to the spark igniter. The oxidizer flows around the outside of the plasma plug into the igniter chamber where it impinges with the fuel flow just downstream of the plasma plug.

II, A, Task I - Igniter Design and Fabrication (cont.)

The basic low P_c igniter design is the same as that of the high P_c igniter. The dimensions are changed to accommodate the requirements of the low P_c design point.

b. Heat Transfer, Stress and Materials Analyses

Hydraulic, heat transfer, stress and ignition characteristics of the high P_c igniter were analyzed to verify igniter design. The results of these analyses are discussed below.

(1) Hydraulic Analysis

The igniter system which was analyzed is shown in Figure 2.* The hydraulic analysis consisted of using the design parameters listed in Table I (such as valve inlet pressure and fuel and oxidizer flowrates) to size critical dimensions of the basic igniter design, i.e., coolant and igniter hot gas throat dia. The throat dia required to satisfy design flowrates were calculated by evaluating feed line pressure drops and heat transfer and friction losses within both the coolant and hot gas circuits. The stagnation pressures at certain system key points were iterated by varying geometry until initial design flowrate requirements were met.

Two igniters were analyzed, one designed for a nominal thrust of 25 lbF and one designed for 50 lbF. The igniter design P_c was 300 psia in the zero back pressure case. The system was evaluated at a core mixture ratio of 35:1 and an overall mixture ratio of 5.0. The two igniters analyzed only differed in thrust chamber throat area and fuel injector spacer size.

*Note that, although this figure shows the igniter in the spark configuration, the hydraulic analysis also applies to the plasma pulse configuration.

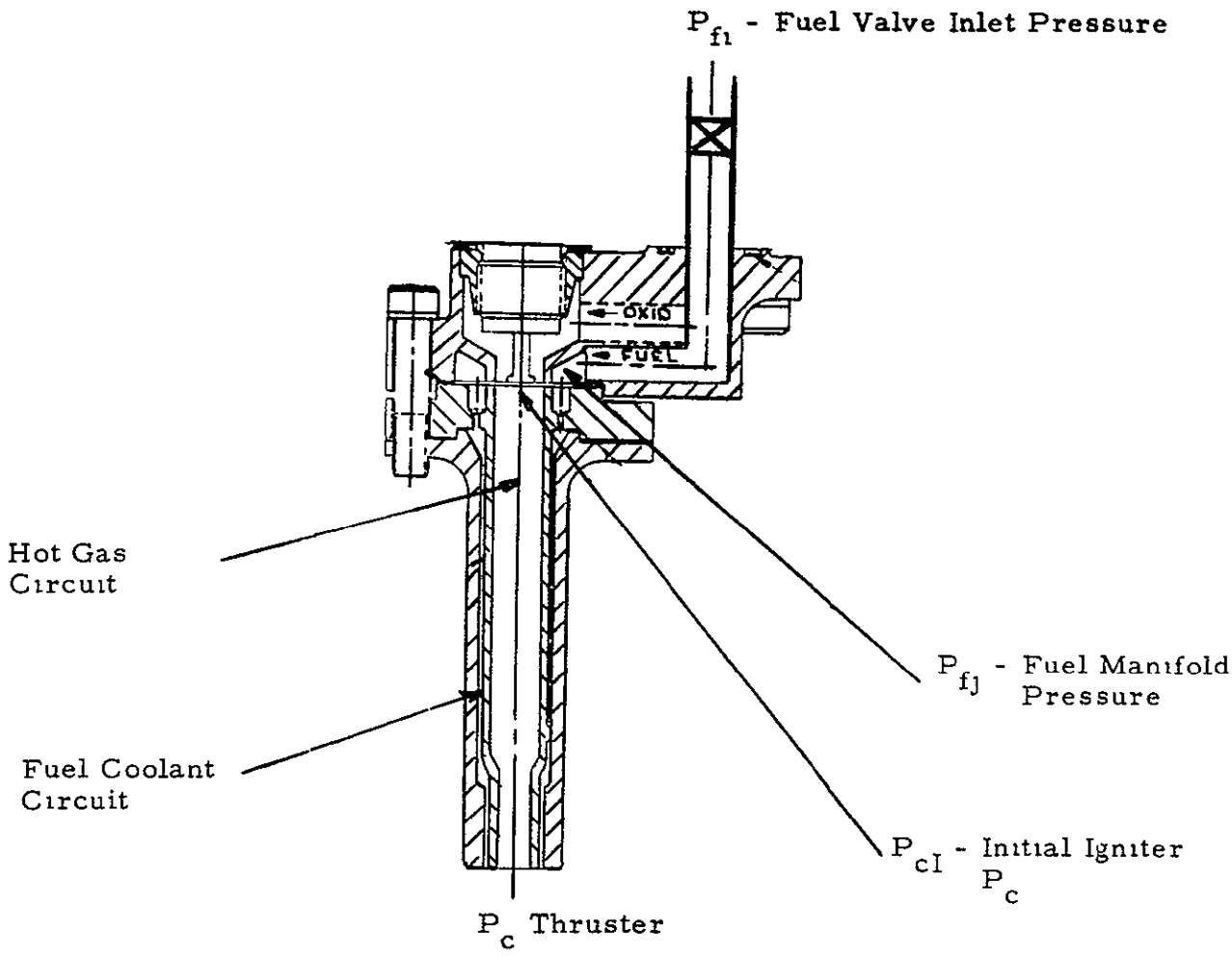

Figure 2. High P_c Spark Igniter Nomenclature

TABLE I

DESIGN CRITERIA - HIGH P_c O_2/H_2 SPARK IGNITER

	Nominal Thrust Level Igniter-Only Mode	
	50 lb	25 lb
Oxygen Inlet Pressure	375 psia	375 psia
Oxygen Inlet Temperature	540°R	540°R
Hydrogen Inlet Pressure	375 psia	375 psia
Hydrogen Inlet Temperature	540°R	540°R
Oxygen Flow Rate	0.125 lb/sec	0.0623 lb/sec
Hydrogen Flow Rate		
Igniter Core	0.00357 lb/sec	0.00179 lb/sec
Coolant	0.0124 lb/sec	0.0107 lb/sec
Total	0.025 lb/sec	0.0125 lb/sec
Mixture Ratio		
Overall	5	5
Igniter Core	35	35
Exhaust Temperature	5000°R	5000°R
Spark Gap	0.050 in.	0.050 in.
Spark Rate	500 sps	500 sps
Spark Energy	10 millijoules/ spark	10 millijoules/ spark
Minimum Ignition Pressure	17 psia	17 psia
Maximum Ignition Pressure	110 psia	110 psia

II, A, Task I - Igniter Design and Fabrication (cont.)

An important objective of the analysis was to evaluate the effect of varying back pressure on igniter flowrates and mixture ratio as the back pressure at the main engine injector face varies from 0 to 300 psia. The technique used was to assume throat inlet stagnation pressures and to determine whether the resulting flowrate satisfied the initial valve inlet pressure of 375 psia. Another important consideration was the effect of nozzle thermal expansion on the annular coolant flow passage. All sizing was based upon the use of Nickel 200 as the igniter material with a thermal expansion coefficient of 9.1×10^{-6} in./in./°F.

In the case of back pressure equal to zero, a normal sonic compressible flow equation was used to check flowrates through the fuel coolant orifice and the hot gas and coolant throats (Equation 1).

$$\dot{W}_{sonic} = (A)\ (C_d)\ (P_o) \sqrt{\left(\frac{g}{RT_o}\right)\left(\frac{2}{\gamma + 1}\right)^{\frac{\gamma + 1}{\gamma + 1}}} \qquad (1)$$

The feed line losses were calculated and the fuel manifold pressure determined from $P_{fJ} = P_{fi} - \Delta P_{feed\ line}$. (Igniter terminology used in this discussion is explained in Figure 2.) The design coolant flowrate was checked by the use of Equation (1). The pressure drop across the fuel inlet gap to the hot gas circuit was calculated and the initial igniter P_c determined. In order to size the hot gas circuit throat, the Rayleigh and Fanno line pressure losses had to be evaluated from the flow metering gap to the throat inlet. The Rayleigh line loss is the stagnation pressure loss associated with the heat transfer effects in a duct of constant area and is the locus of points on an enthalpy-entropy diagram defined by the momentum equation, continuity equation, and the equation of state. The Fanno line loss is the

stagnation pressure loss associated with friction effects in a duct of constant area and stagnation enthalpy and is the locus of points on an enthalpy-entropy diagram defined by the energy equation, the continuity equation, and the equation of state. It is necessary to calculate both Rayleigh and Fanno line pressure losses for the hot gas and coolant circuits because both heat transfer and friction effects are significant; e.g., the temperature rise for the hot gas circuit was from 540°R to 4430°R. After subtracting these losses from initial igniter P_c, the throat dia required for the hot gas circuit design flowrate could be calculated from the sonic flowrate using Equation (1). The Rayleigh and Fanno line pressure losses were also evaluated for the coolant circuit. In this analysis, it was assumed that a normal shock standing between the coolant orifice exit and the throat inlet would adjust the pressure as required for continuity with two choked orifices in series. The other major design consideration was thermal expansion. Throat expansion and the effect is has in reducing the coolant passage flow area were considered in the design analysis.

The case in which the main injector face is at P_c = 300 psia requires a more complex analysis. The analytical method which was used employed the subsonic compressible equation, Equation (2), in a

$$\dot{W} = (A)\ (C_d)\ (P_o) \sqrt{\left(\frac{2g}{(\gamma - 1)\ RT_o}\right)\left(\frac{P_s}{P_o}\right)^{\frac{2}{\gamma}} - \left(\frac{P_s}{P_o}\right)^{\frac{\gamma + 1}{\gamma}}} \qquad (2)$$

process of iteration. First, oxidizer and fuel manifold pressures and an initial value of igniter P_c were assumed. Igniter injector flowrates were calculated and Rayleigh and Fanno line pressure losses were proportioned to these new values. The hot gas throat inlet stagnation pressure was calculated

by subtracting these losses from the igniter face pressure and the compressible subsonic flow equation was used to find the throat flowrate. This value was compared with the previously computed injection flowrate. When these two flowrates converged, the value for P_{fJ} was used to determine the corresponding fuel coolant flowrate. This process was also one of iteration. A value was assumed for the coolant throat inlet stagnation pressure and the flowrate calculated. After evaluating the Rayleigh and Fanno line losses, the fuel orifice outlet pressure was determined and used along with P_{fJ} to determine the orifice flowrate. The orifice flowrate and throat flowrates were compared and the process repeated until convergence occurred. Finally, a check was made to determine whether the final fuel manifold pressure was in agreement with the final total fuel flowrate and the corresponding fuel line pressure drop.

The results of the analysis are listed in Table II. In addition to providing the data required to size the fuel coolant circuit and the hot gas circuit, the analysis indicated that the presence of 300 psia back pressure caused a reduction in overall mixture ratio for the 25-lbF igniter, i.e., from 5.0 to 4.37. Similarly, the 300 psia back pressure caused a reduction in the core mixture ratio for the 50-lbF igniter, i.e., from 35 to 33.5. Both mixture ratio shifts are modest and are not expected to limit igniter operation.

An investigation of the effect of differing igniter design chamber pressures on general system design parameters was also made. These results are summarized in Table II. It was found that system stagnation pressures and flowrates were directly proportional to igniter P_c within one percent.

TABLE II

FLOW CHARACTERISTICS - HIGH P_c SPARK IGNITER

$P_{cThruster}$ (psia)	P_{FI} (psia)	P_{OI} (psia)	P_{fJ} (psia)	P_{oJ} (psia)	P_{cign} (psia)	$\dot{W}_{oign}$ (lb/sec)	$\dot{W}_{fign}$ (lb/sec)	$\dot{W}_{fcool.}$ (lb/sec)	MR Over-all	MR Core	V_{oJ} ft/sec	V_{fJ} ft/sec	$V_{cool.}$ ft/sec
	F = 25 lb												
0	375	375	368.5	369	299	0.0625	0.001785	0.0110	5	35	135	1415	2845*
300	375	375	373	373	345	0.0395	0.00120	0.00785	4.37	35	95	940	2060
0	625	625	615	615	500	0.104	0.00298	0.0183	5	35	135	1415	2845
0	125	125	123	123	100	0.0208	0.000595	0.00367	5	35	135	1415	2845
	F = 50 lb												
0	375	375	345	350	300	0.125	0.00357	0.0214	5	35	285	1750	1940**
300	375	375	362	362	337	0.0895	0.00267	0.0134	5	33.5	181	1160	1810
0	625	625	570	578	500	0.208	0.00595	0.0341	5	35	285	1750	1940
0	125	125	116	118	100	0.0417	0.00119	0.0069	5	35	285	1750	1940

*At 25 lbF, the coolant stream temperature rise was assumed to be 420°F.
**At 50 lbF, the coolant stream temperature rise was assumed to be 140°F.

II, A, Task I - Igniter Design and Fabrication (cont.)

(2) Heat Transfer

The steady state heat transfer characteristics of the high P_c igniter were calculated using the Aerojet HEAT computer program. This program is used for the analysis of regenerative cooling. The temperature and pressure, as well as transport properties, Mach number, etc., of the coolant are determined at each station along the contour by a "marching" calculation that proceeds in the direction of the coolant flow. A variety of coolant passage geometries may be treated. The heat flux and wall temperature are also calculated at each station; two-dimensional enhancement of heat conduction in channel walls is accounted for by means of a fin-type equation.

The computer calculated results for the new 25-lbF high P_c igniter are summarized in Table III. The indicated wall temperature is 2015°F which is considered too high for a safe operating point. The indicated high temperatures are contrary to the experimentally measured igniter wall temperatures obtained with the original igniter. Therefore, the original igniter design was run on the computer as a check. The results, listed in Table III, show the wall temperature to be above the melting temperature of Hastelly X but in fact the measured temperature was on the order of 700°F. This apparent discrepancy will be studied in detail during cold flow MR profile testing of the igniter.

In the interest of providing a cooler igniter operating point, the igniter MR was raised to 50 and the coolant flow increased to give an overall MR of 4. This case was run in the computer and the results are included in Table III. The results show this operating point to be considerably cooler from a steady state operating standpoint. It may prove to be desirable to change the igniter design point to the MR = 50 case. However, it is recommended that a decision be withheld pending the results of the cold flow MR profile measurements.

TABLE III

HEAT TRANSFER COMPUTER RESULTS

Thrust Level	Igniter Core MR	Igniter Overall MR	Wall Mat'l	Throat Gas Side Temp. °F	Throat Coolant Side Temp. °F	Wall ΔT (°F)	Coolant Velocity (ft/sec)	Heat Flux (Btu/in^2-sec)
25	35	5	Nickel (New Ign.)	2015	1661	354	1800	5.41
25	35	5	Hastelloy X (Original Igniter)	2630	1996	639	389	2.57
25	50	4	Nickel	1436	1142	294	930	3.92

II, A, Task I - Igniter Design and Fabrication (cont.)

The properties of the materials considered for the igniter chamber are listed in Table IV. Based on the results of the heat transfer analysis, TD Nickel would be the ideal selection for a long-life igniter due to its higher strength. However, Nickel-200 was selected for this program because of cost and availability considerations.

(3) Ignition Characteristics

The maximum and minimum ignition pressure limits for both the high and low P_c igniter designs were predicted on the basis of existing Aerojet ignition data. The maximum cold flow pressure at which ignition can occur in either the plasma pulse or spark igniter is controlled by the output voltage of the power supply and the spark or plasma arc electrode spacing. The relationship between the breakdown voltage and the pressure and electrode spacing are defined by Paschen's Law as indicated in Figure 3. Both the spark and plasma pulse power supplies will deliver 30,000 volts. Therefore, the limiting value of pressure times the electrode space (P·G) is about 5.5.* The curve of pressure versus electrode spacing shown in Figure 4 was drawn using this value of (P·G).

The design values of the spark and plasma electrode spacing and the corresponding cold flow pressures for both the high and low P_c igniter designs are indicated on Figure 4. Note that both the spark and plasma pulse low P_c igniter designs fall well below the ignition limit line and, therefore, breakdown failure is not expected to occur with the low P_c igniter designs. This is not the case, however, for the high pressure spark and plasma pulse igniters. The steady state cold flow chamber pressure for these igniters is 100 psia. The spark igniter design point occurs at the 100 psia level, placing it 10 psi below the ignition limit. This may appear to give only a small margin of safety. Note, however, that the unit ignites

*Oxygen and air are assumed to behave similarly.

TABLE IV

TYPICAL PROPERTIES OF CANDIDATE IGNITER NOZZLE MATERIALS

Alloy	Condition	Test Temp (°F)	Conductivity (Btu/ft-hr-°F)	Yield Strength (ksi)	Fatigue Strength (ksi)	Ignition Temp (°F)
TD Nickel	Stress relieved bar stock	1700	28.3	--	--	--
		1800	--	18	12 (10^7 cycles)	
		2000	--	15	11 (10^7 cycles)	
A-200 Nickel	Annealed	1200	35.0	10	--	2650
Hastelloy X	Solution annealed at 2150°F and rapid air cooled	1800	16.2	16	15 (10^6 cycles)	2300

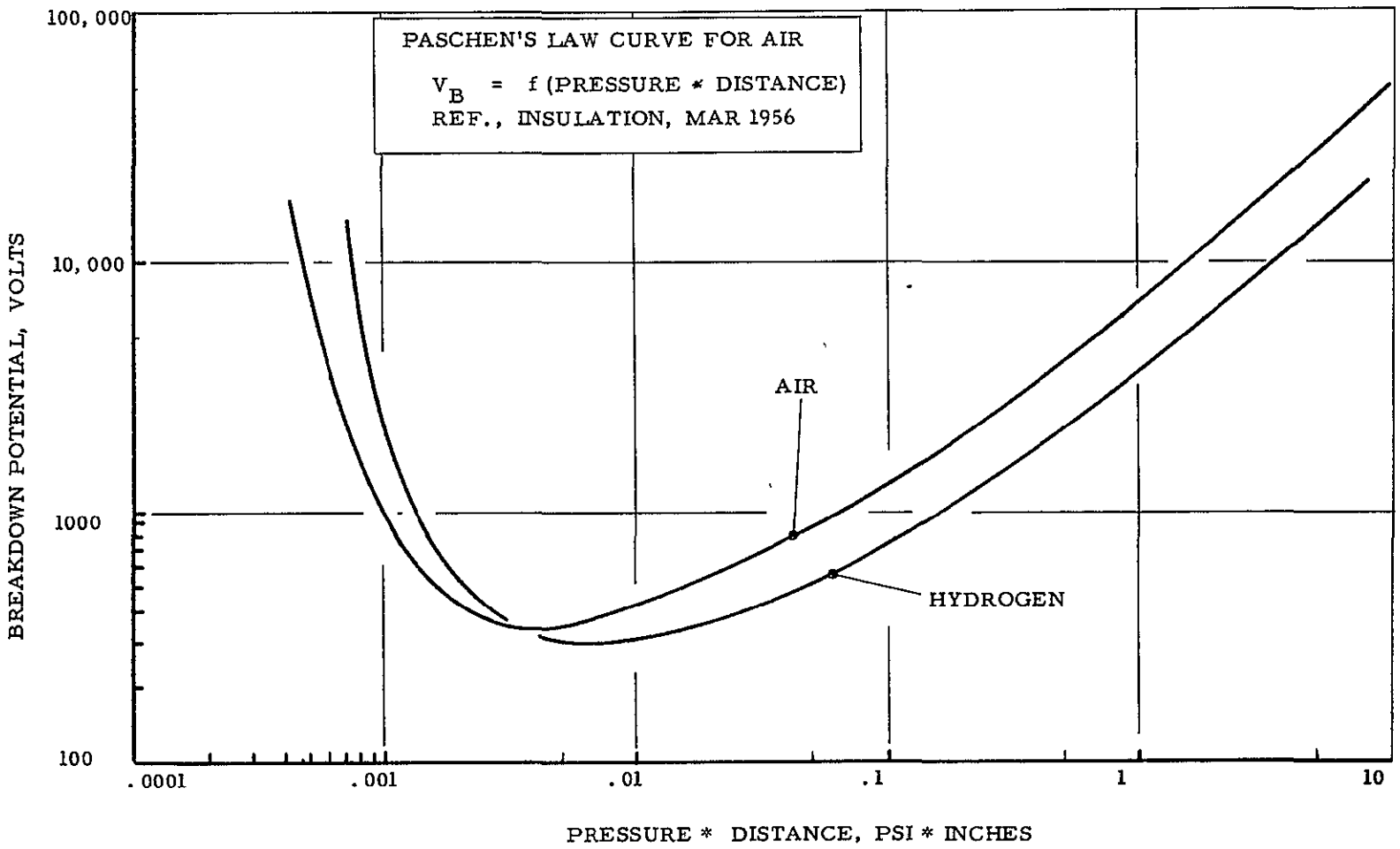

Figure 3. Paschen's Law Curves

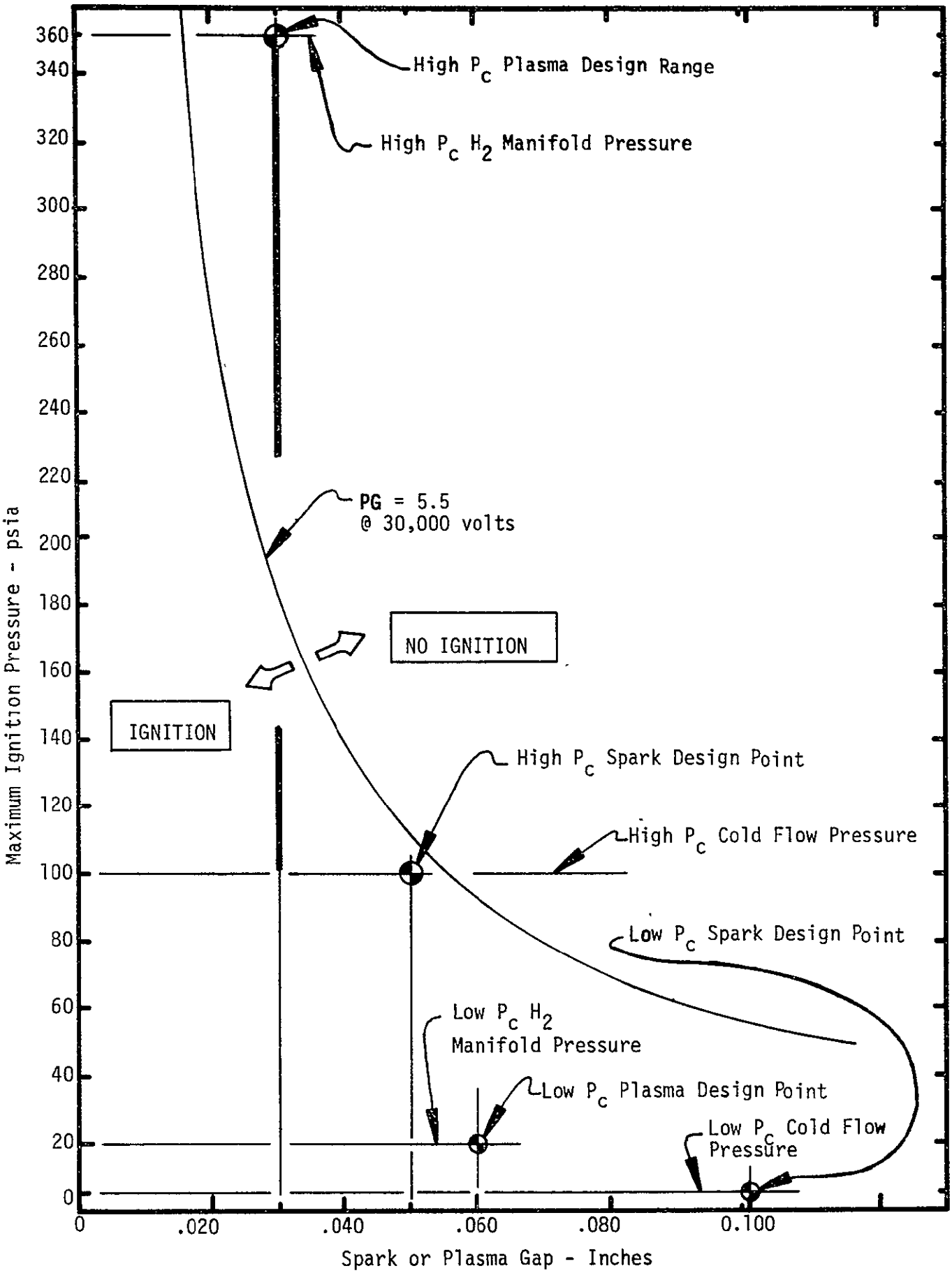

Figure 4. High & Low P_c Igniter Maximum Ignition Pressure Limits

during the initial flow transient when pressures in the chamber are well below the 100 psia steady state level indicated on Figure 4. The actual location of the pressure limit line and the desired margin of safety will be investigated during the test program.

The high pressure plasma pulse igniter design is unique in that it is shown to have a design range rather than a design point. The hydrogen cold flow pressure around the electrode can be made to vary from the hydrogen manifold supply pressure (360 psia) down to the igniter chamber pressure cold flow pressure (100 psia) by varying the size of the hydrogen plasma injection orifice. The small orifice gives high steady state cold flow pressures, an undesirable feature as indicated in Figure 4, but enhanced hydrogen-oxygen mixing in the igniter chamber. A large orifice, on the other hand, results in low cold flow pressures, and a large margin of safety relative to the steady state igniter pressure limit, but decreased igniter chamber mixing. The small orifice data obtained previously may be complimented with large orifice data during the test program. Note that the plasma pulse igniter, like the spark igniter, actually experiences ignition during the flow transient and 100% ignition success has been achieved with plasma even under the worst small orifice design conditions, i.e., 360 psia cold flow pressure.

The minimum ignition pressure limit is determined by the flame quenching phenomena. Therefore, it is independent of the ignition technique. Rather, it depends on the mixture ratio, the igniter chamber dia and, to a lesser extent, the propellant temperature, as indicated in Figure 5. The critical value of the flame quenching parameter (P·D) is about 5.0 at a mixture ratio of 35. This value of (P·D) was used to draw the pressure versus chamber dia curve shown in Figure 6.

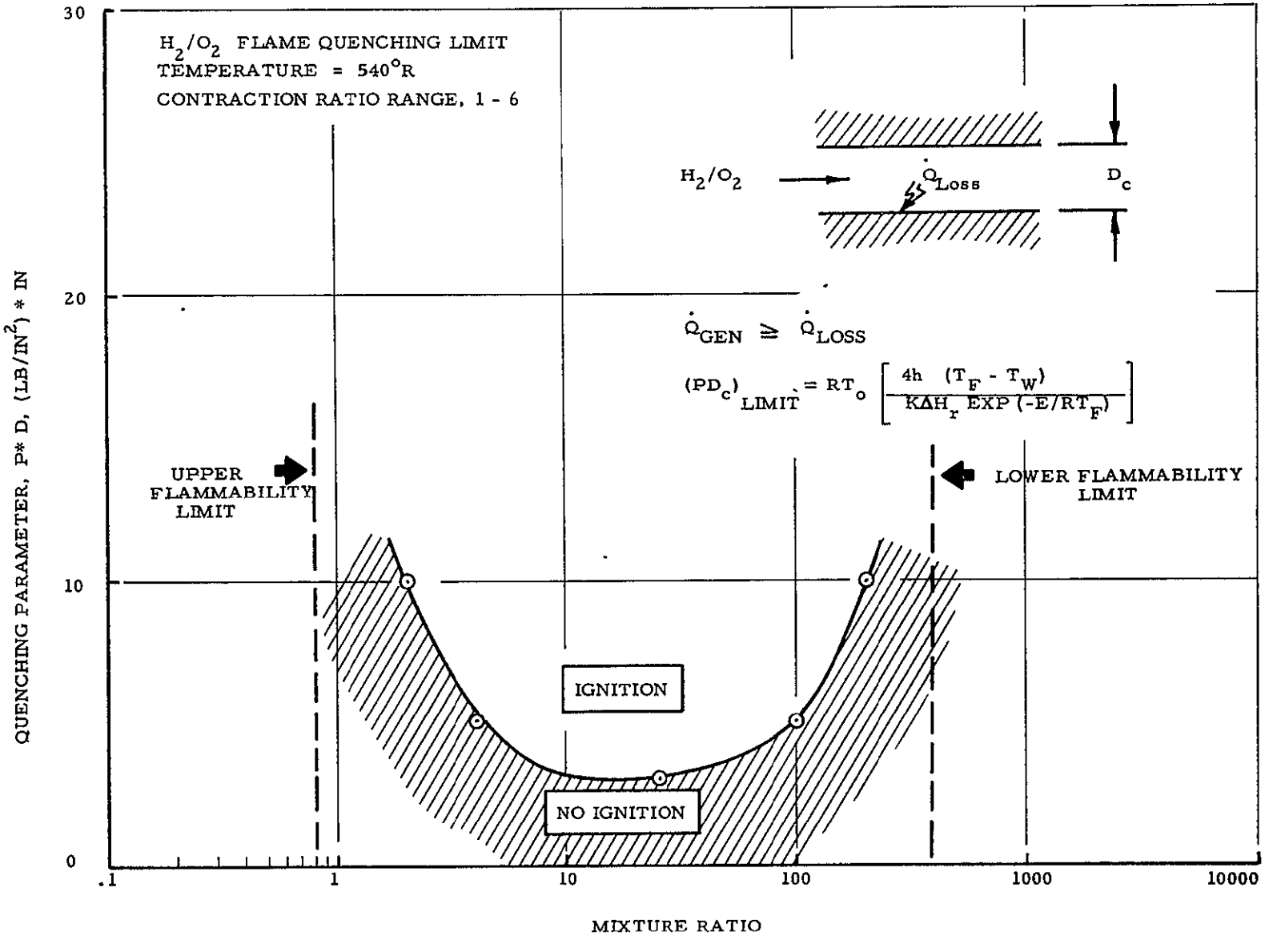

Figure 5. Effect of Mixture Ratio on Flame Quenching Parameter

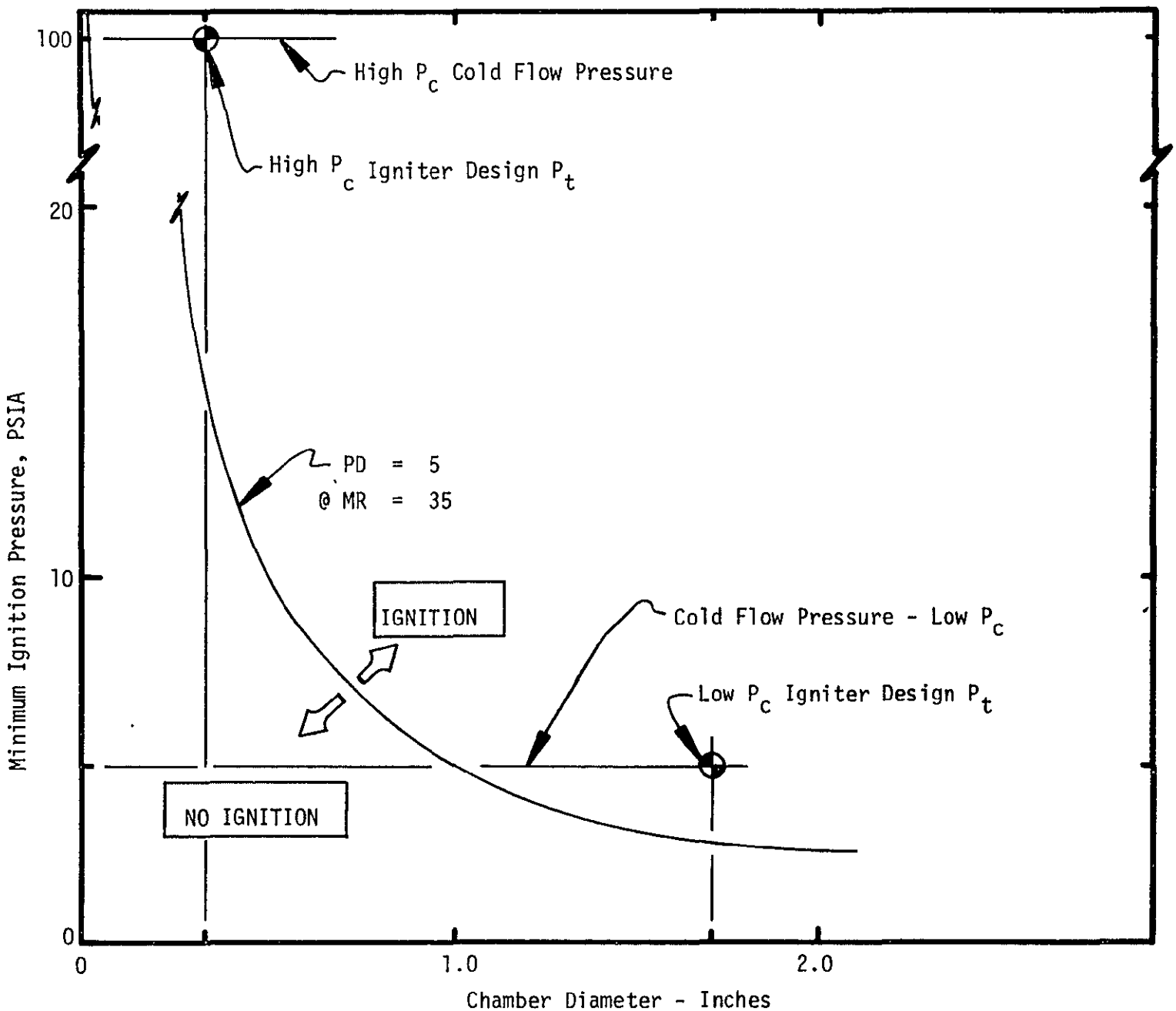

Figure 6. High & Low P_c Igniter Minimum Ignition Pressure Limit

II, A, Task I - Igniter Design and Fabrication (cont.)

The design chamber dia and cold flow pressures for the high and low P_c igniters are indicated in Figure 6. Note that the high P_c igniter design cold flow pressure is a factor of 6 higher than the quenching pressure and, therefore, ignition failures due to flame quenching are not expected to occur with the high P_c igniter. The low P_c igniter design cold flow pressure is about double the quenching pressure although the absolute magnitude of the margin of safety is small. This problem has been anticipated in the test program by providing for throttling of the flow to determine this flame quenching pressure precisely.

An analysis of the effect of the igniter mixture ratio of disproportionably varying the propellant inlet temperatures was made to determine its effect on engine ignition. This was done by holding both the oxidizer and fuel inlet pressures constant at 375 psia and letting first the fuel temperature vary and then letting the oxidizer temperature vary. The results of this calculation are plotted in Figure 7. The core MR is seen to vary from MR = 20 to MR = 52. The igniter exhaust temperature will be adequate for reliable engine ignition over this range of mixture ratios. Previous work has indicated ignition should occur up to an igniter mixture ratio of about 75. However, the MR = 20 condition will result in a high igniter chamber temperature. This problem will be investigated further.

c. High P_c Igniter Drawings

The preparation of the drawings for the spark and plasma igniters for the high chamber pressure design point was completed. These drawings were reviewed in detail during the Design Review held in Sacramento on August 5 and 6, 1970. As a result of this review, these drawings were approved by E. A. Edelman, contingent upon the execution of several minor changes. These changes were made and the drawings were released to initiate fabrication of the high P_c spark and plasma pulse igniters.

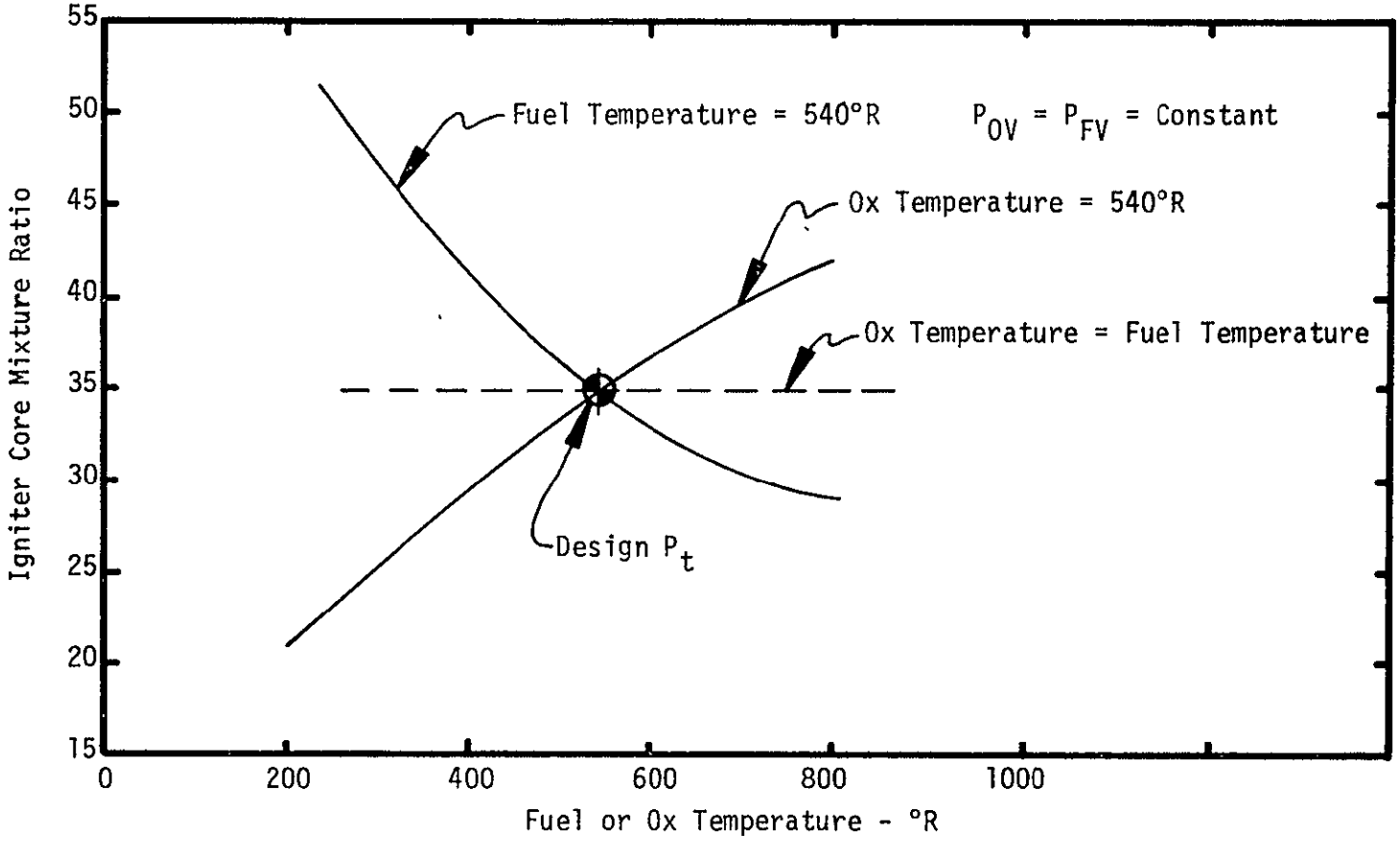

Figure 7. Effect of Propellant Inlet Temperature on Igniter Mixture Ratio

The assembly drawing for the spark igniter for the high P_c design point is shown in Figure 8. The propellant flow circuits are indicated. Note that the hydrogen flow is split, with part entering the combustion chamber just downstream of the spark electrode and part entering the combustion chamber cooling circuit.

The assembly drawing for the plasma pulse igniter for the high P_c design point is shown in Figure 9. In this igniter the hydrogen flow is split differently, with part entering the combustion chamber after flowing through the plasma plug and part entering the combustion chamber cooling circuit.

The assembly drawing for the impinging coaxial injector for the high P_c design point is shown in Figure 10. This injector is designed to accept both the spark and plasma pulse igniters on a completely interchangeable basis.

A drawing for the heat sink combustion chamber for the high P_c design point is shown in Figure 11. The TCA described in Figures 10 and 11 will be used in the evaluation of the igniters described in Figures 8 and 9 in the Igniter-Only, Igniter-Complete Thruster and Ignition Durability Test Subtasks.

d. Low P_c Igniter Drawings

The preparation of the drawings for the spark and plasma pulse igniters for the low chamber pressure design point was completed. These drawings were reviewed in detail during the aforementioned Design Review. As a result of this review, these drawings were approved by E. A. Edelman, contingent upon the execution of several minor changes. These changes were made and the drawings were released to initiate fabrication of the low P_c spark and plasma pulse igniters.

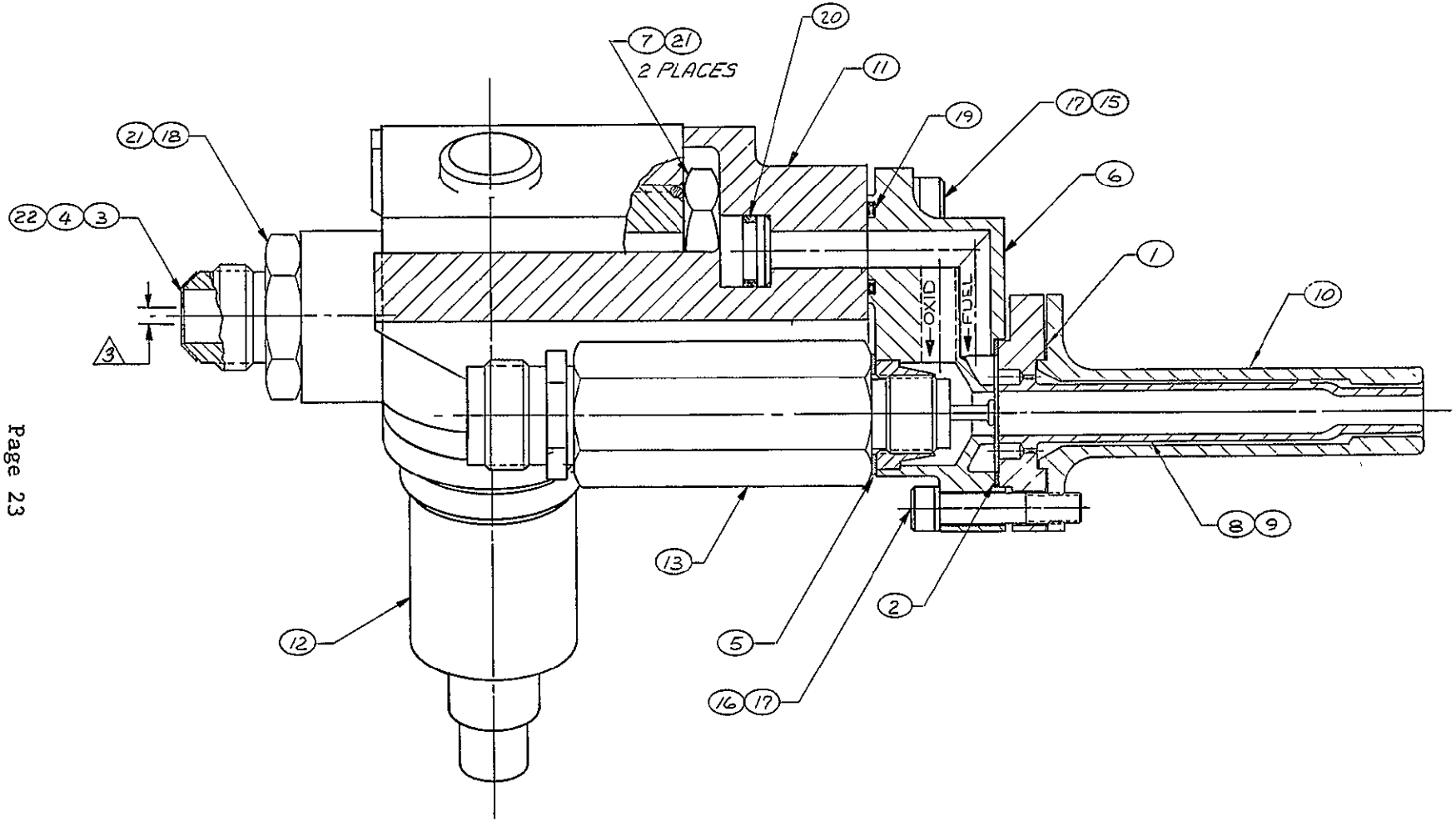

Figure 8. Spark Igniter for the High Chamber Pressure Design Point

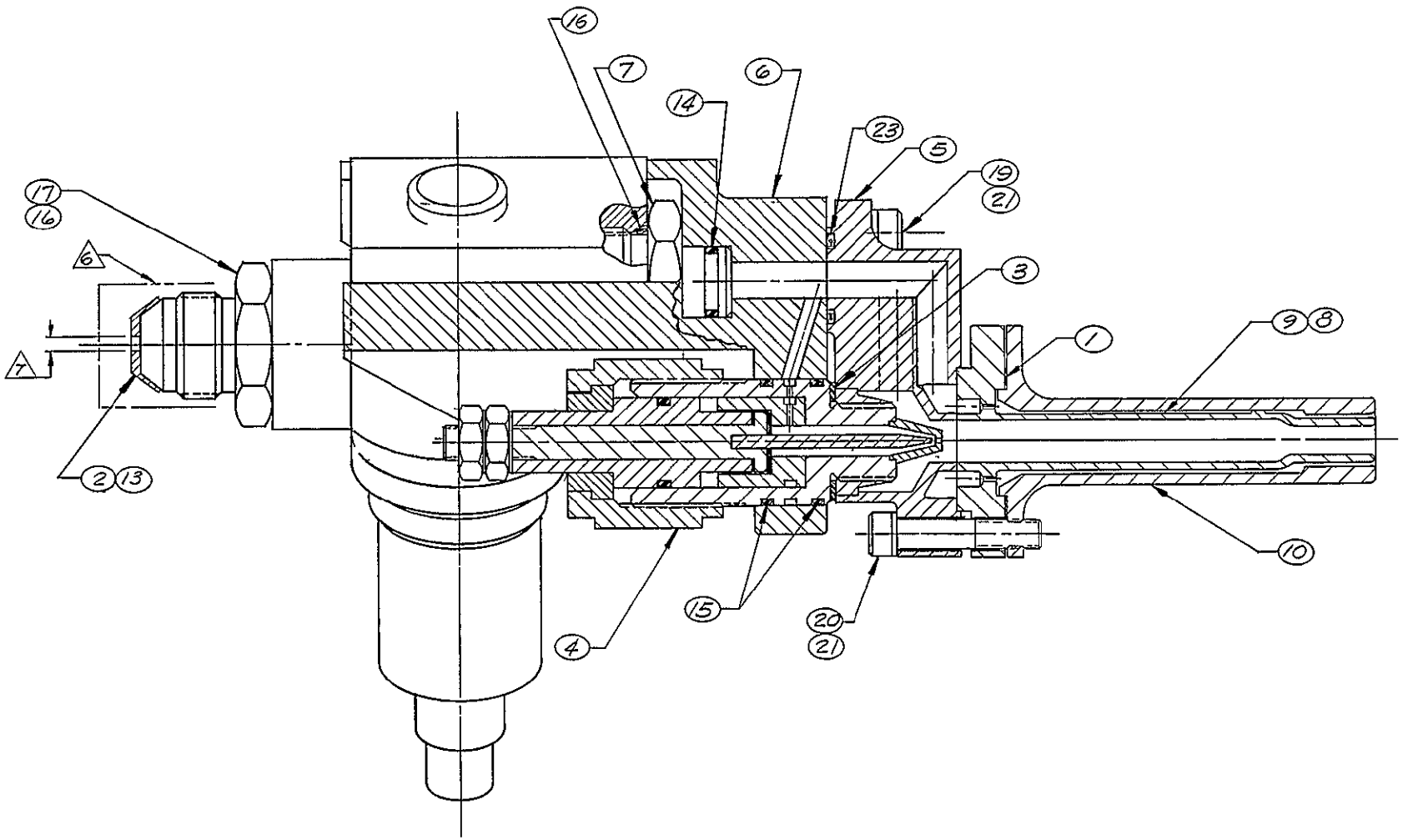

Figure 9. Plasma Pulse Igniter for the High Chamber Pressure Design Point

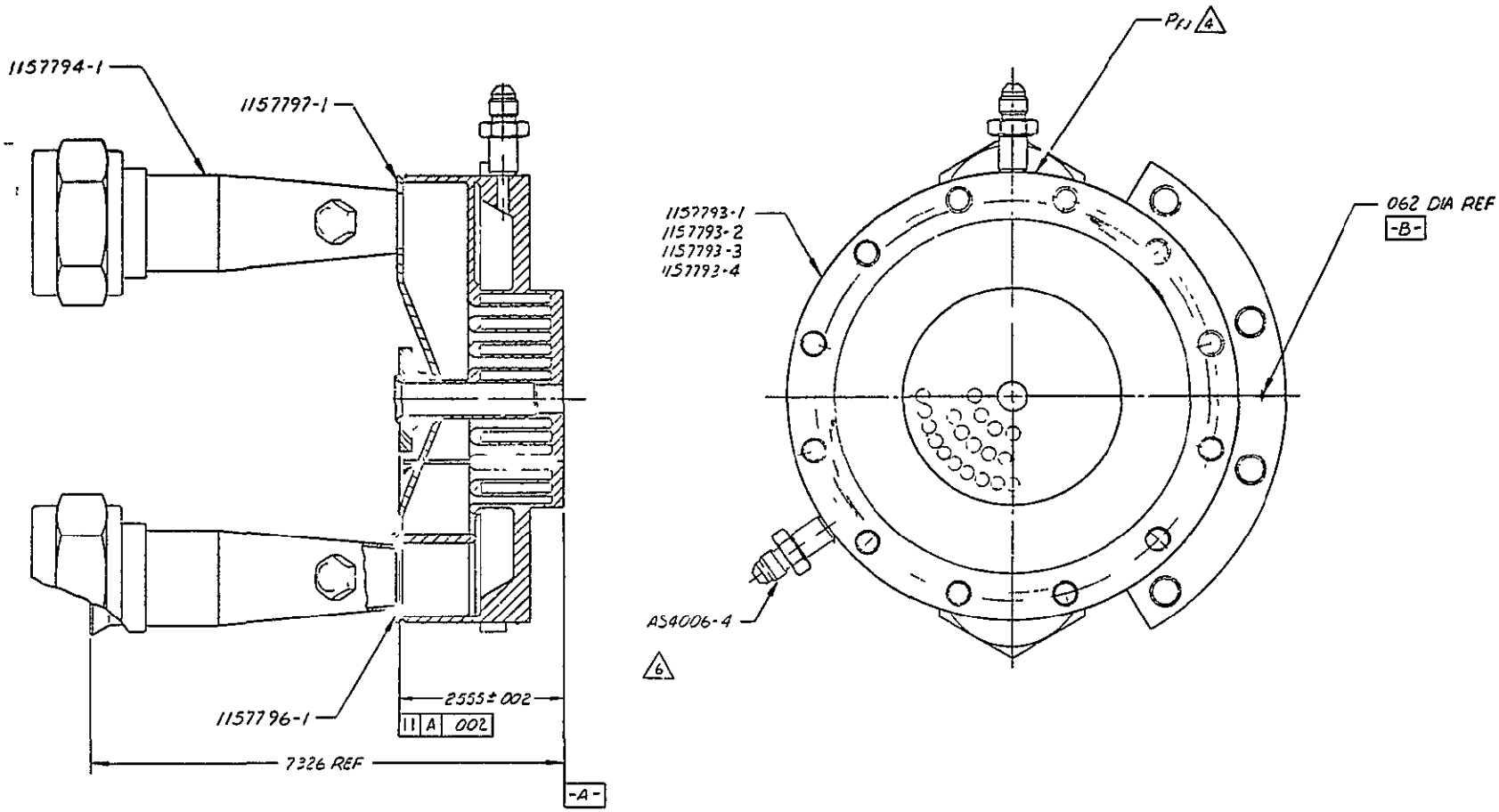

Figure 10. Injector for the High Chamber Pressure Design Point

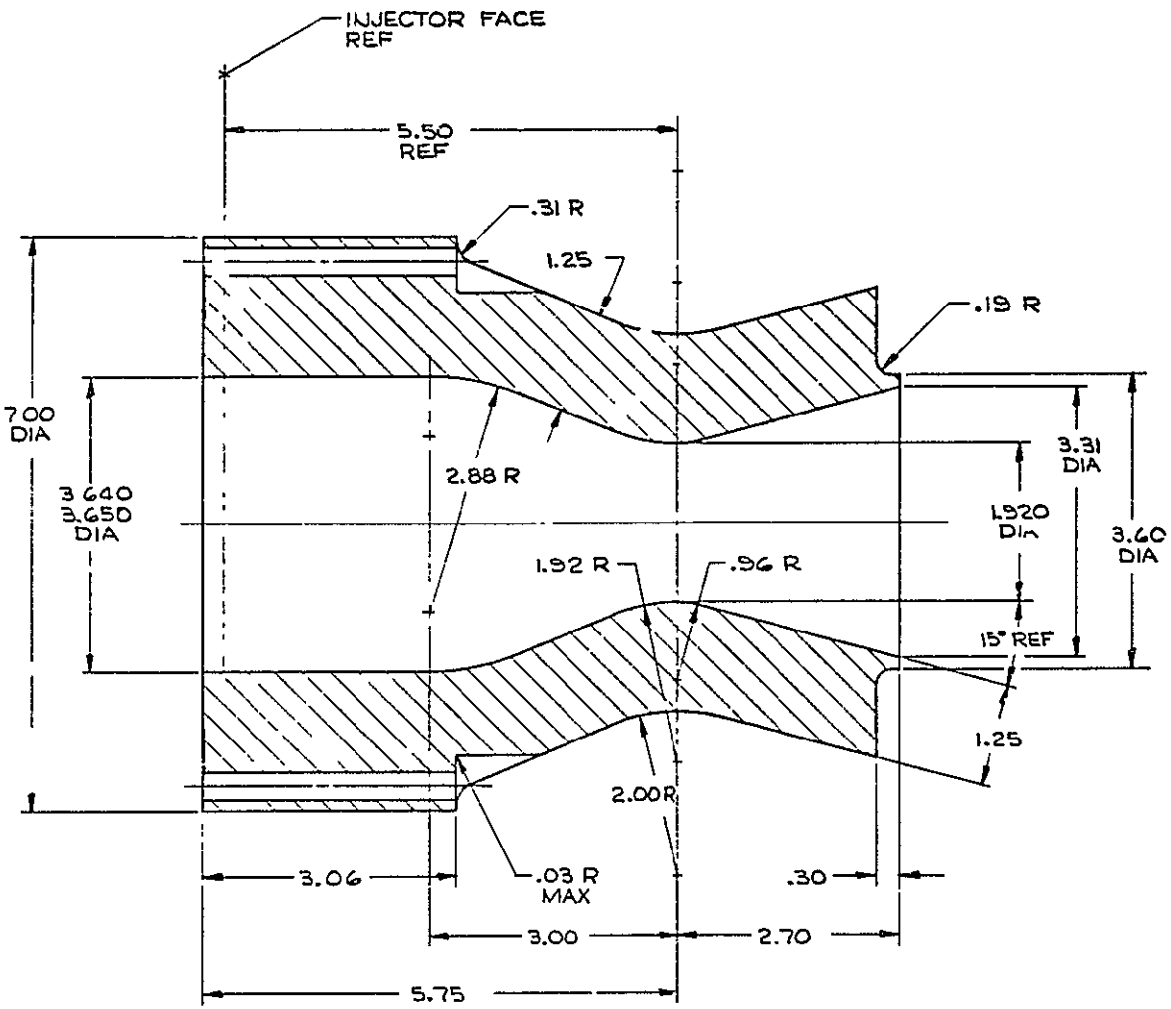

Figure 11. Combustion Chamber for the High Chamber Pressure Design Point (15 in. L*)

II, A, Task I - Igniter Design and Fabrication (cont.)

The assembly drawings for the spark and plasma pulse igniters for the low P_c design point are shown in Figure 12. The propellant flow circuits are the same as those of their high P_c counterparts.

The assembly drawing for the coaxial injector for the low P_c design point is shown in Figure 13. This injector is designed to accept both the spark and plasma pulse igniters on a completely interchangeable basis.

A drawing for the uncooled combustion chamber for the low P_c design point is shown in Figure 14. The TCA described in Figures 13 and 14 will be used in the evaluation of the igniters described in Figure 12 in the Igniter-Complete Thruster and Ignition Durability Test Subtasks.

2. Fabrication

The fabrication of the spark and plasma pulse-igniters for the high P_c design point was completed. The fabrication of the companion igniters for the low P_c design point was nearing completion at the end of the report period.

B. TASK II - IGNITER TESTS

The Task II test program will be conducted to obtain preliminary design data for both spark and plasma electrical ignition systems. It is divided into six major subtasks: Analysis; Electrode Durability Tests; Igniter-Only Tests; Igniter-Complete Thruster Tests; Ignition Durability Tests; and Igniter EMI Tests.

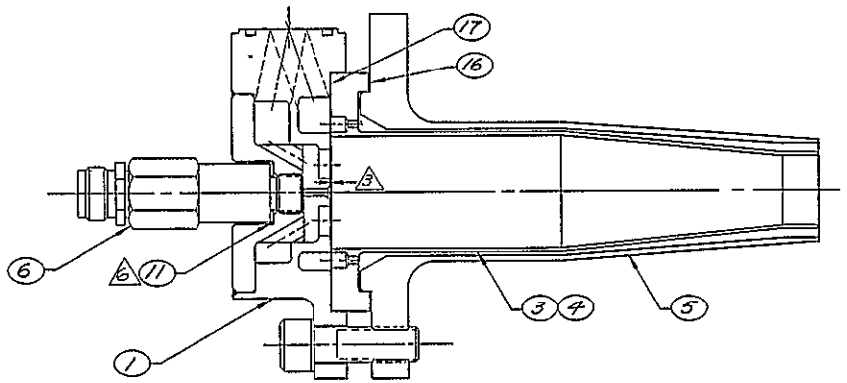

-9 ASSEMBLY

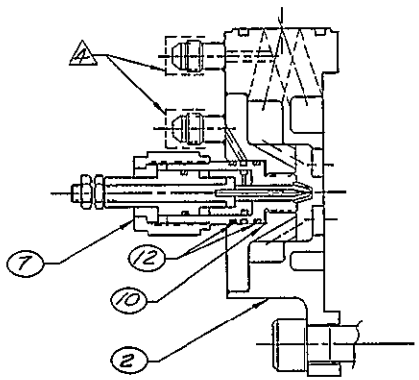

-19 ASSEMBLY

Figure 12. Spark and Plasma Pulse Igniters for the Low Chamber Pressure Design Point

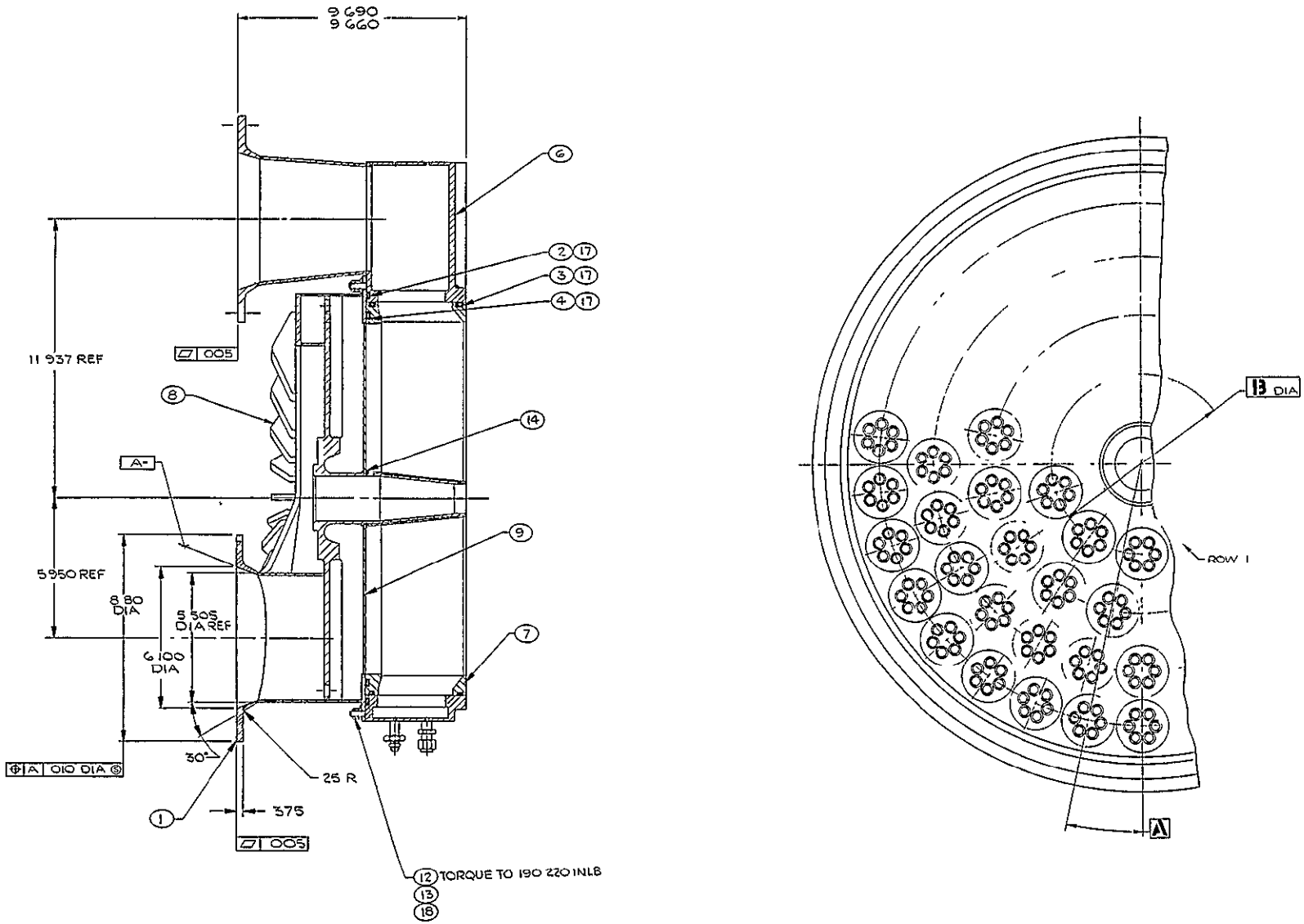

Figure 13. Injector for the Low Chamber Pressure Design Point

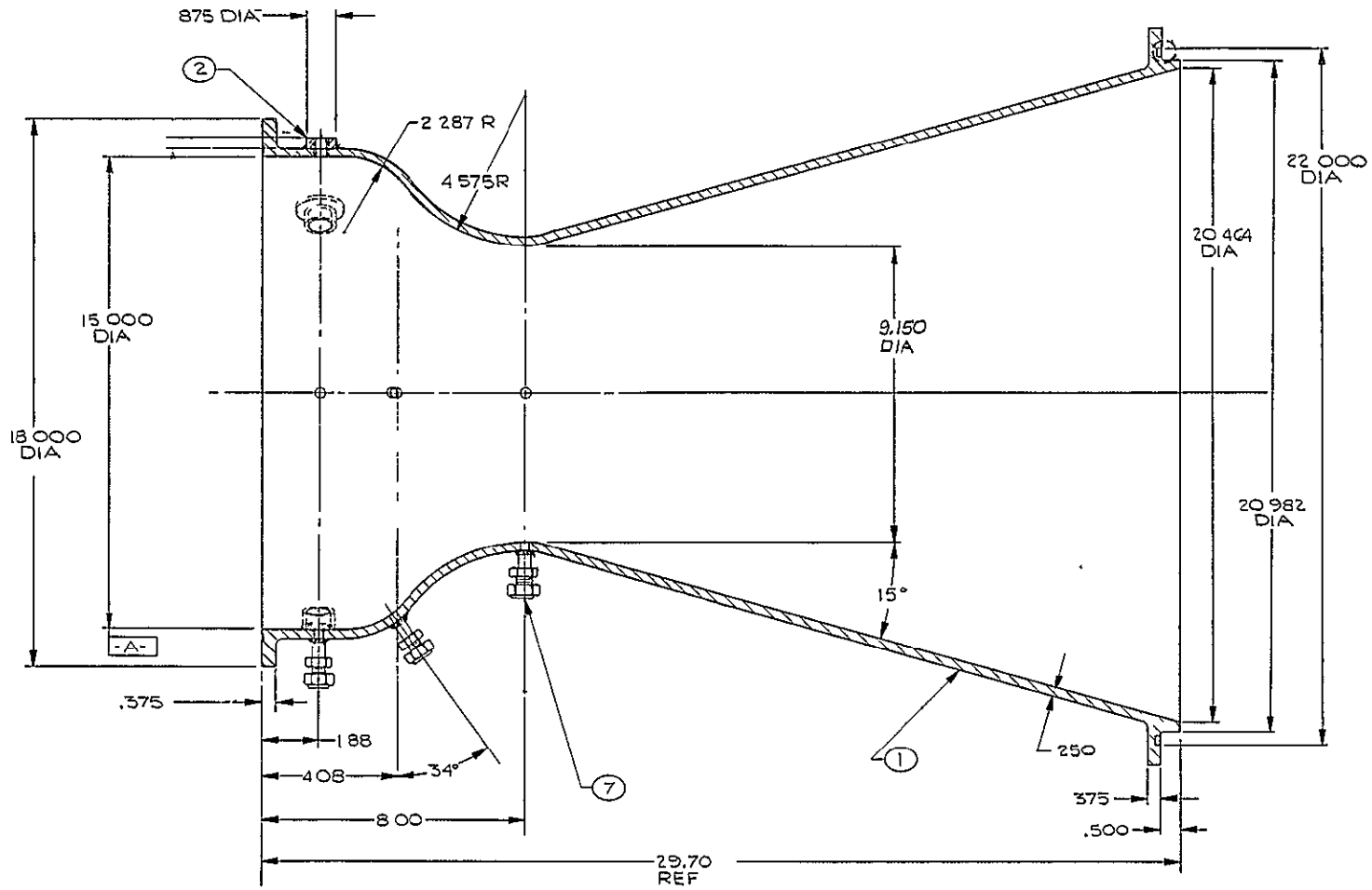

Figure 14. Combustion Chamber for the Low Chamber Pressure Design Point

II, B, Task II - Igniter Tests (cont.)

1. Ignition Analysis

There are two basic considerations which govern engine ignition system requirements: Ignition delay and ignition over-pressure. Both conditions must be minimized. The ignition delay must be minimized as it affects engine response and ignition over-pressure. The ignition over-pressure must be minimized as it affects engine durability and fatigue life. These factors cannot be controlled without knowledge of the relationship between them and the ignition system and engine operating conditions. Therefore, the purpose of the ignition analysis task is to develop a technique for predicting the effect of engine inlet conditions on ignition delay and over-pressure. This is being done by the development of a computerized analytical model of GO_2/GH_2 pilot torch ignition. The results of this analysis will be compared to, and modified by, the experimental test results so that a computerized simulation of GO_2/GH_2 engine ignition will be available for use during the preliminary design phase. Progress on this task has included definition of the engine ignition model, checkout of the Turbulent Mixing and Combustion Computer Program, and checkout and modification of the Transient Flow Computer Program. Each of these items is discussed below.

a. Engine Ignition Model

The problem to be solved is that of determining the ignition delay and ignition over-pressure of a GO_2/GH_2 rocket engine which is ignited by a pilot torch flame as illustrated in Figure 15. High temperature igniter gases are injected into the main chamber at high velocities, in most cases supersonic, where it rapidly mixes with the lower velocity cold engine flow. Ignition of the engine flow is brought about by the exchange of energy between the hot igniter exhaust gases and the cold engine gases. Ignition is indicated by the occurance of chemical reaction within the engine flow. The factors which determine when ignition will take place are the

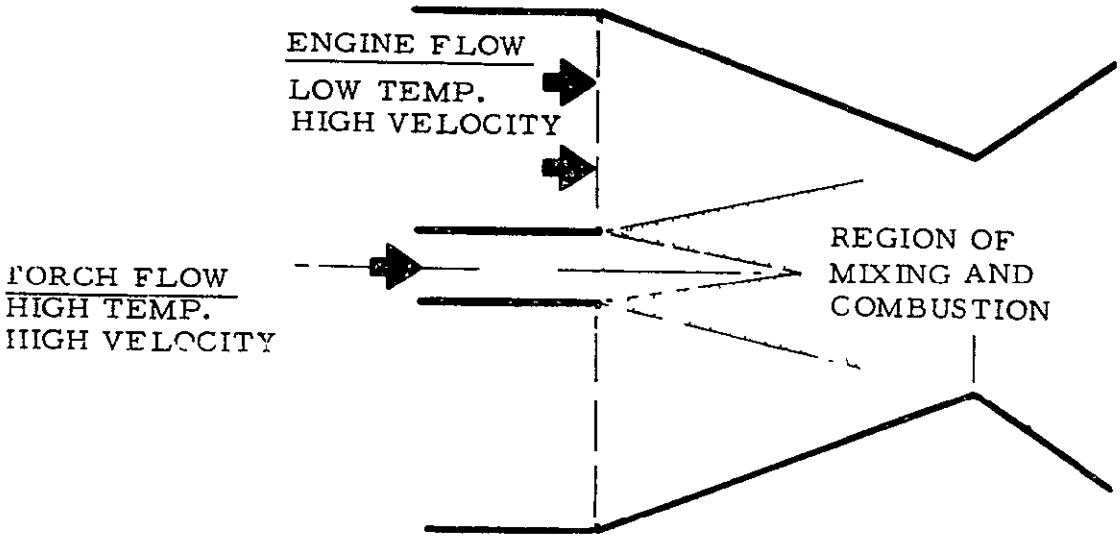

IGNITION CONTROLLED BY

MIXING

- RELATIVE VELOCITIES
- IGNITER SIZE AND GEOMETRY

COMBUSTION

- REACTION KINETICS
- TEMPERATURE
- MIXTURE RATIO
- GAS VELOCITIES

Figure 15. Oxygen/Hydrogen Engine Torch Ignition Mechanism

rate of mixing and the rate of combustion. The mixing rate is controlled by the igniter and main engine relative velocities and the igniter size and geometry. The rate of combustion is controlled by the reaction kinetics which, in turn, are dependent upon the igniter exhaust temperature and mixture ratio, and the main engine mixture ratio, temperature and cold flow pressure.

The problem becomes one of describing the engine flow conditions and their interaction with the igniter exhaust flow as a function of time as these are rapidly changing during the start transient. The engine cold flow conditions are chronologically described by a transient flow computer program which calculates the engine flowrate, mixture ratios, and cold flow chamber pressures for given propellant inlet conditions. The torch exhaust conditions are determined by the igniter inlet conditions, which are held constant with time, and the engine cold flow pressure. Interaction between the igniter exhaust jet and the engine flow is described by a separate steady state turbulent mixing and combustion computer program which calculates the exchange of mass, momentum, and energy.

Determination of the ignition time requires that the transient flow computer calculations be couples with the steady state turbulent mixing and combustion computer calculations. Ideally, the mixing program could be input to the transient flow program as a sub-routine which would calculate the ignition conditions at each point in the transient. However, the magnitude of the effort required to do this is beyond the scope of the current program. Therefore, coupling of the computer programs will consist of running the mixing program at a sufficient number of pre-selected engine operating conditions to define a set of ignition limit curves as shown in Figure 16. These curves will then be input to the transient flow computer program as tables. At each point in the transient the engine conditions will be compared to the tables to determine when ignition occurs.

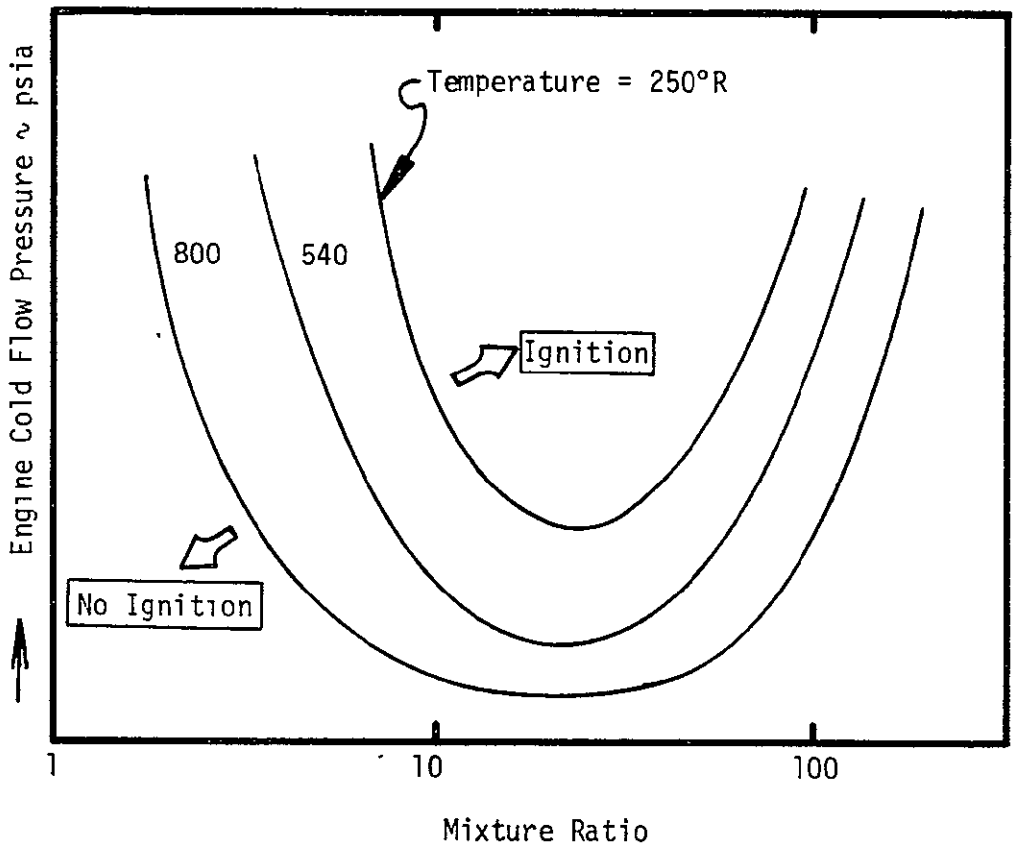

Figure 16. Calculated GO_2/GH_2 Torch Ignition Limits

The ignition overpressure is also calculated at each point in the transient. The overpressure is calculated on the basis of (1) a rapid constant volume explosion and (2) a Chapman-Jouget detonation wave. The reason for including the detonation wave calculation is that the peak pressure behind the wave front can be as much as three times greater than that calculated on the basis of the constant volume explosion. The detonation wave overpressure calculation provides an upper limit of the ignition overpressure.

A flow diagram of the calculational procedure is shown in Figure 17. The engine configuration, valve characteristics, and propellant inlet conditions are input to the transient flow computer program which starts calculating the transient mixture ratio cold flow chamber pressure and cold flow propellant temperatures. These parameters are then used to calculate the ignition overpressure and to determine whether or not an ignition condition exists. If no ignition condition exists, the program continues to calculate the cold flow transient. If an ignition condition exists, the ignition delay and ignition overpressure are printed out and the program terminates.

The results of this analytical task will be the generation of curves of ignition delay and ignition overpressure versus propellant inlet conditions and valve lead/lag conditions.

b. Transient Flow Computer Program

The Transient Flow Computer Program calculates the propellant densities in the injector manifold and chamber volumes using an Adams integration technique to solve a set of simultaneous differential equations which describe the change in propellant density with time. The manifolding and chamber pressures are calculated from the density using the ideal gas law.

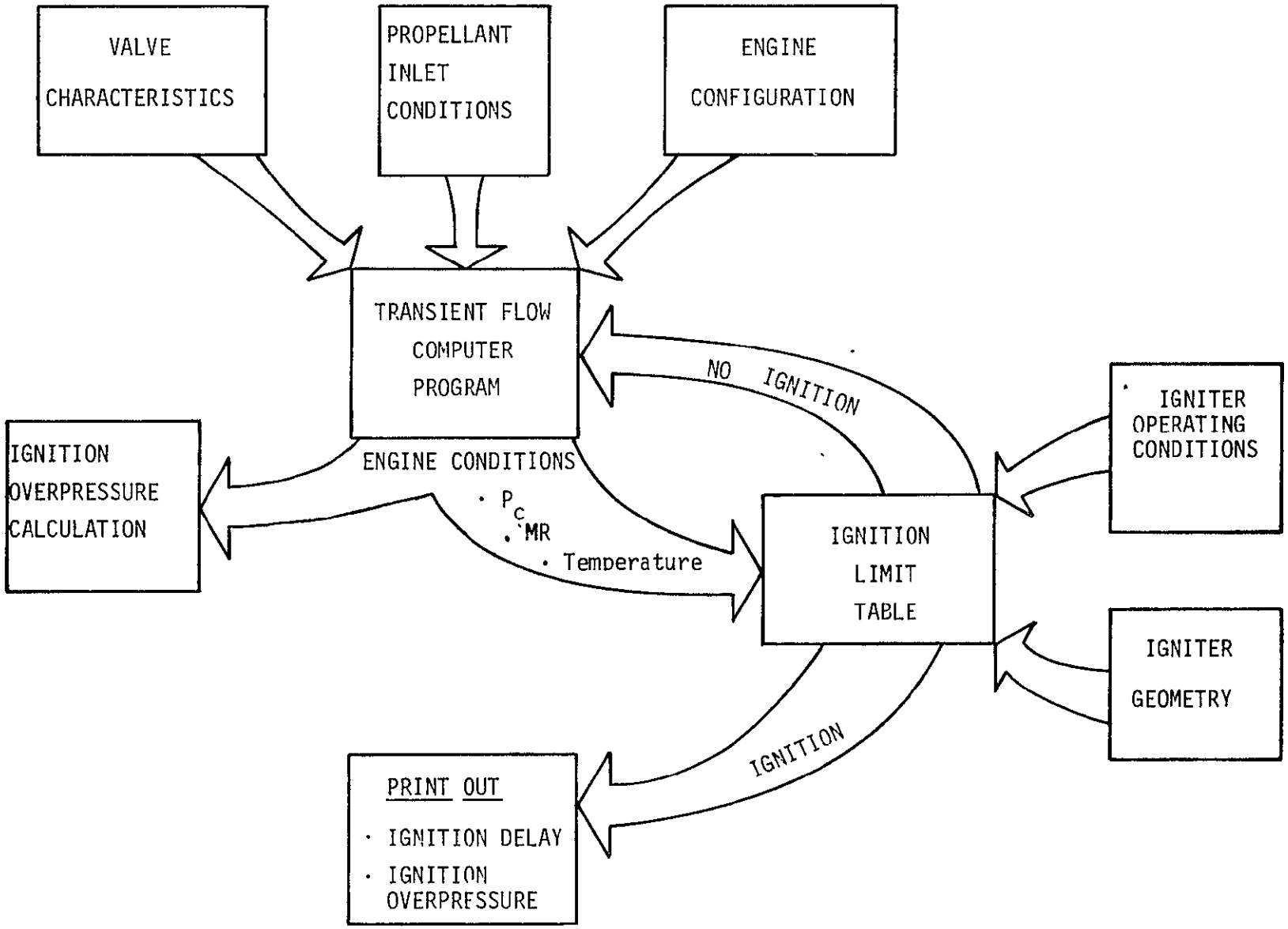

Figure 17. Engine Ignition Model - Flow Diagram

II, B, Task II - Igniter Tests (cont.)

The flowrates into and out of the volumes are described by the isentropic compressible flow equation. Allowance is made for choked, i.e., sonic, flow conditions.

The required engine and operating input conditions are listed in Table V. The program can handle any desired valve opening characteristic or valve lead or lag condition. An example of the program output is shown in Figure 18. This transient was calculated for the high P_c injector and chamber configuration that will be tested during the Igniter-Complete Thruster Test Subtask.

A simultaneous valve opening was used with a 15 msec valve opening time. It is noted that the fuel manifold volume fills faster than the oxidizer manifold which causes a mixture ratio shift to the fuel rich side during the transient. This MR shift may be desirable from some operating standpoints; however, it may not be desirable from an ignition standpoint.

The program originally did not allow for back flow of the leading propellant into the lagging manifold during a lead or lag condition. This did not allow for the proper starting conditions of the lagging propellant and gave erroneous mixture ratios during the early part of the transient. The program was modified to correct this condition. A typical oxidizer lead (hydrogen lag) start is illustrated in Figure 19.

The program was also modified to include calculation of the ignition overpressure assuming a detonation occurs. The detonation overpressure calculation was input to the program as a set of tables of detonation wave pressure ratios versus mixture ratio for selected propellant temperatures.

TABLE V

TRANSIENT FLOW COMPUTER PROGRAM - INPUT PARAMETERS

Valve Characteristics (Fuel & Ox.)

1. Table of area vs % open
2. Start of opening time
3. Full open time
4. Maximum valve area

Operating Conditions

1. Propellant inlet pressure
2. Propellant inlet temperatures
3. Ambient pressure

Engine Characteristics

1. Injector manifold volumes
2. Injector flow area
3. Chamber volume
4. Nozzle throat area

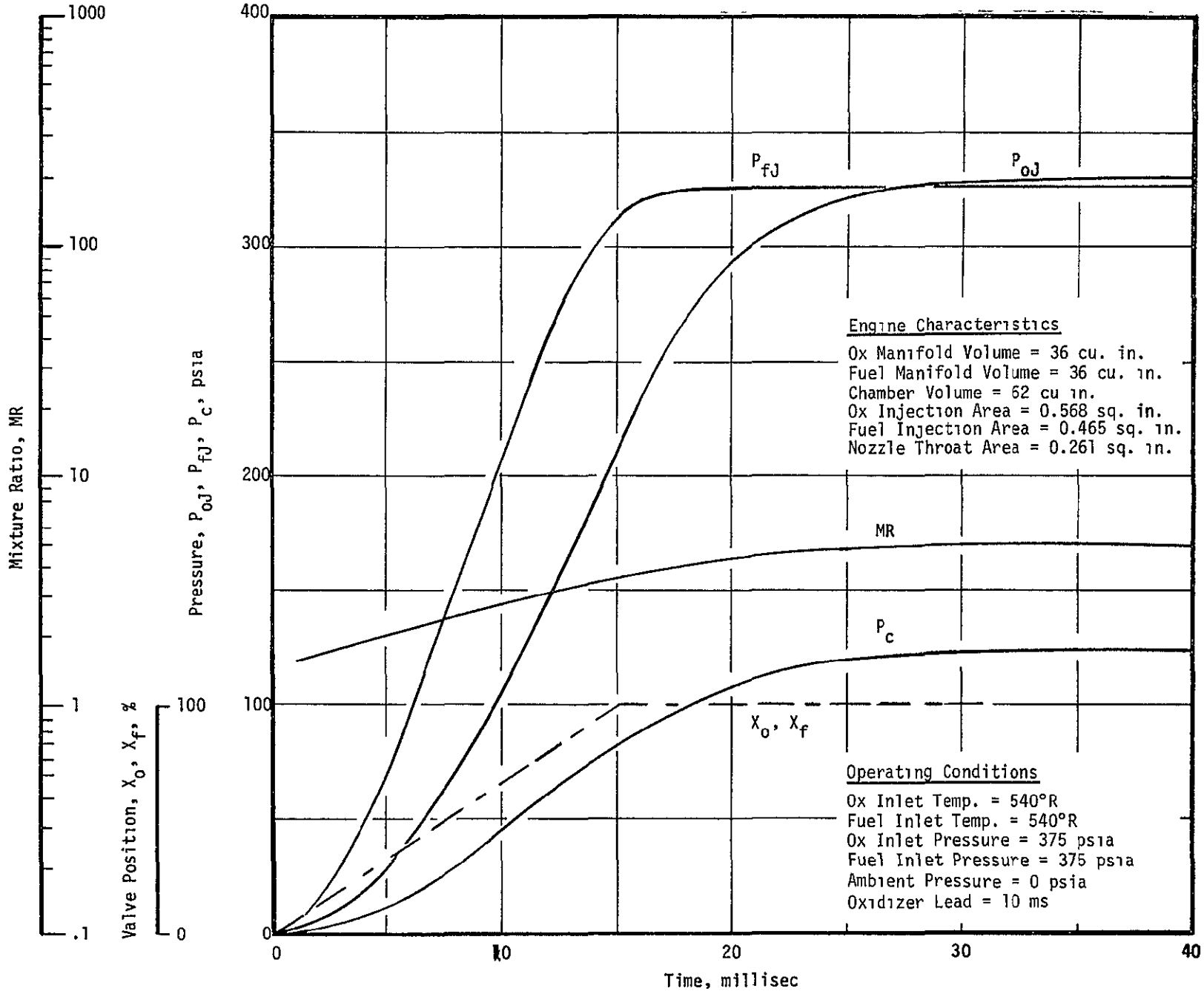

Figure 18. Calculated O_2/H_2 Engine Cold Flow Transient, Simultaneous Start

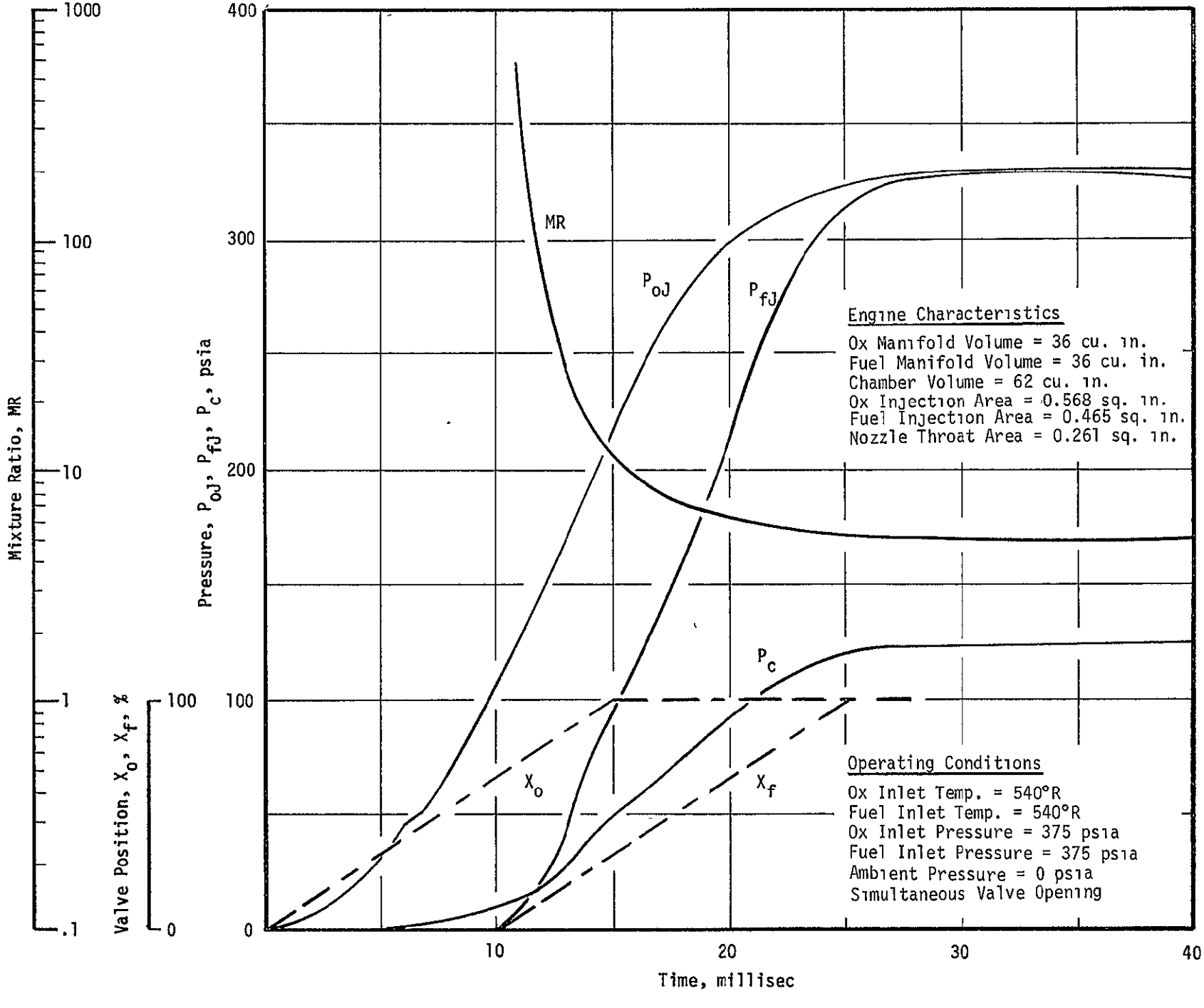

Figure 19. Calculated O_2/H_2 Engine Cold Flow Transient, Oxidizer Lead

These pressure ratios were calculated using the ICRPG ODE Computer Program which calculates the Chapman-Jouget detonation wave properties. The pressure ratio data are plotted in Figure 20 for reference. The initial pressure was found to have a negligible effect on the detonation pressure ratio; therefore, the controlling factors are the propellant temperature and mixture ratio. The detonation wave ignition overpressure is found by extrapolating the table with the MR and propellant temperature to find the pressure ratio which is then multiplied by the current cold flow chamber pressure. This modification was completed. Calculated ignition overpressures for an oxidizer lead (hydrogen lag) start transient are plotted in Figure 21.

c. Turbulent Mixing and Combustion Computer Program

The Turbulent Mixing and Combustion Computer Program calculates the exchange of mass, momentum, and energy between parallel gas streams. The transport of these properties is assumed to be by turbulent diffusion which depends upon the magnitude of the velocity differences and a turbulent eddy viscosity. Molecular transport phenomena are neglected. The injector flow is presumed to provide a uniform gas mixture. The program handles chemical reaction of the mixing flows. The computer program is currently being checked out and the calculation of the ignition limit curves will be started at a later date.

The program has been used to predict the cold flow mixing of the fuel and oxidizer within the high P_c spark and plasma pulse igniter chambers. The results of these calculations are shown in Figure 22.

The plasma pulse igniter results show that the fuel tends to stay toward the center of the chamber leaving a large film of oxidizer along the igniter wall. It should be noted that this is a cold flow condition and that combustion will modify the distribution to some extent.

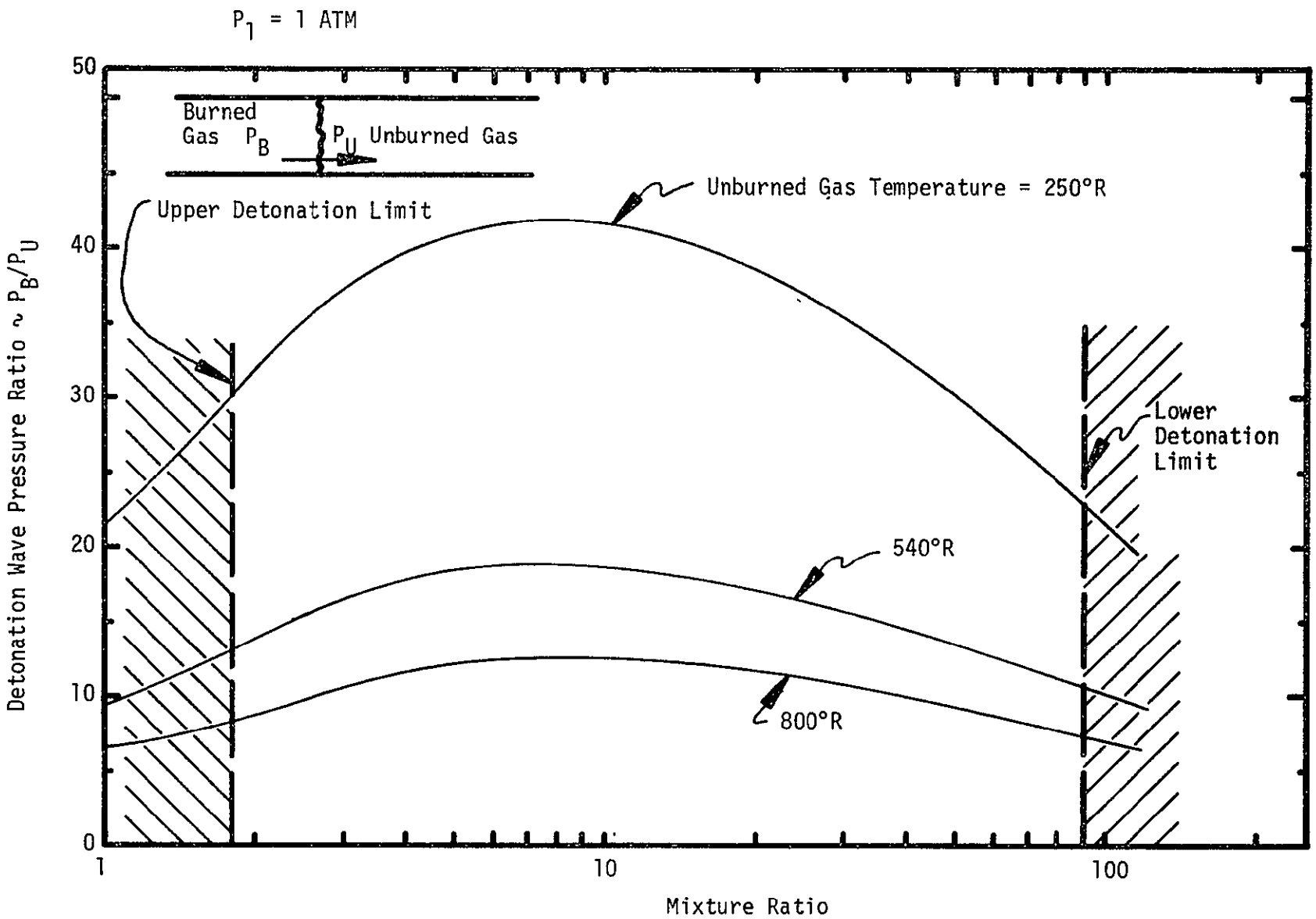

Figure 20. O_2/H_2 Detonation Wave Pressure Ratio VS Mixture Ratio

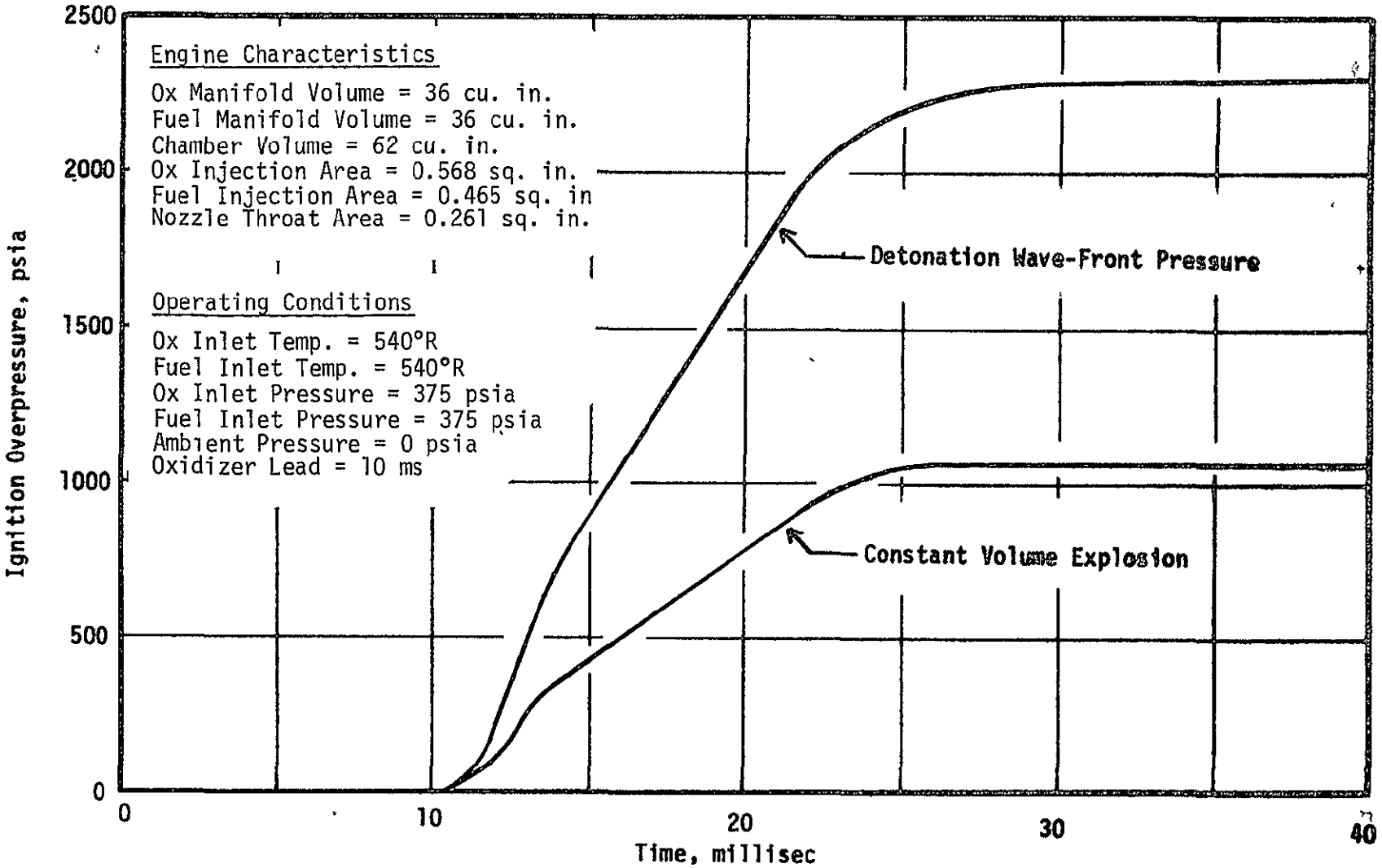

Figure 21. Calculated Ignition Overpressure, Oxidizer Lead Start

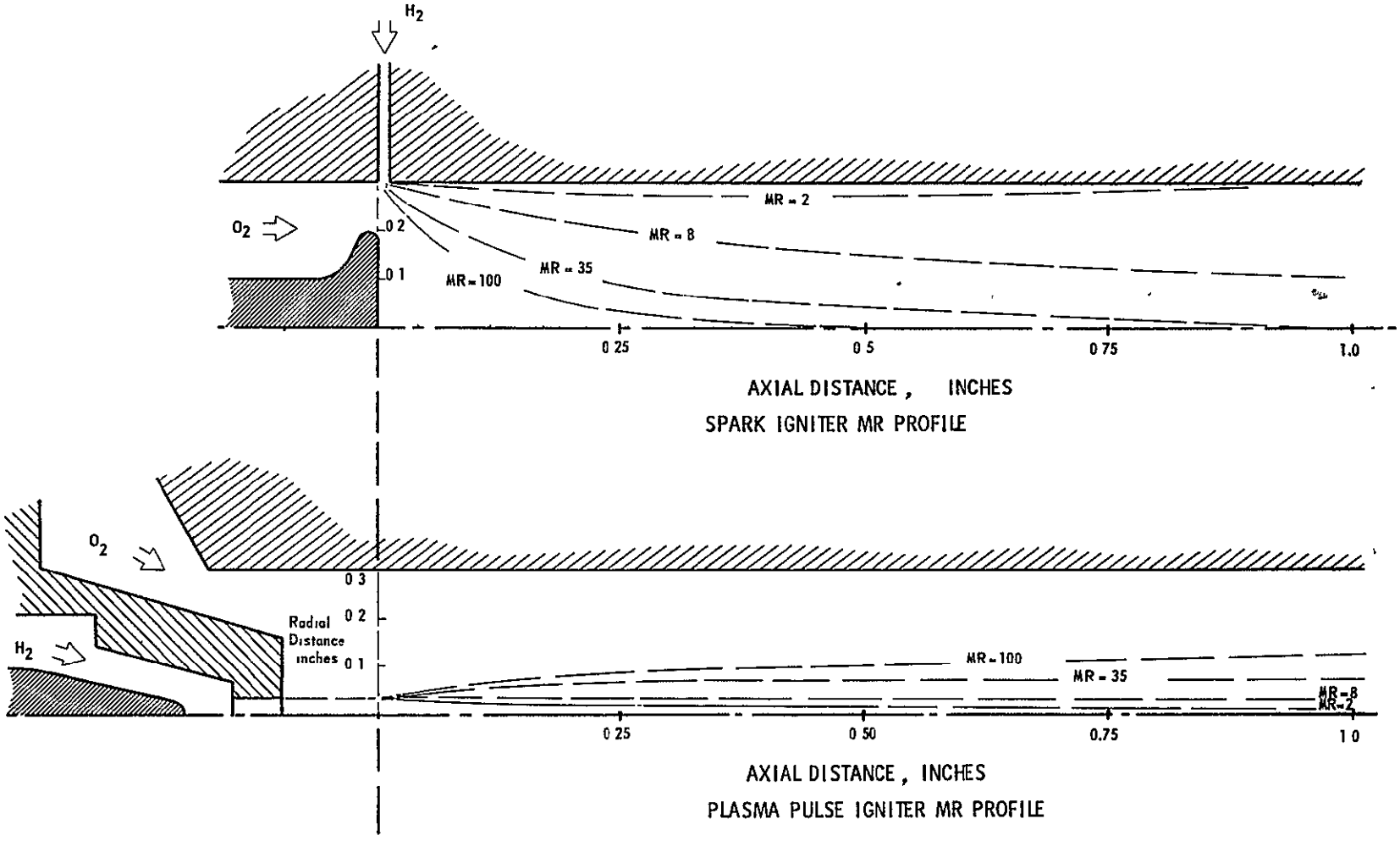

Figure 22. Igniter Mixture Ratio Profiles

The spark igniter results indicate that a thin fuel rich boundary exists along the igniter chamber wall. Because the computer program can only handle axial streams, some assumptions had to be made as to what velocity should be used for the fuel stream which is injected radially. It was decided to use the fuel injection velocity but assume the jet to be rotated 90° because the resultant momentum angle of the combined fuel and oxidizer streams is only 9° away from the wall. The validity of this assumption will be checked out when the MR profiles are measured in the laboratory. The MR profiles can be recomputed on the basis of the experimental results.

2. Test Facility Setup

Four test locations are being used on this program. The Igniter Cold-Flow Calibration Tests are being performed in the Aerophysics Laboratory where the special calibration and mixture ratio survey equipment are located. The Igniter-Only Tests will be performed in Bay 1 of the Physics Laboratory where a new test position for the igniters has been built and activated. The Igniter-Complete Thruster Tests are to be conducted in Bay 7 of the Physics Laboratory. A new test facility, including propellant conditioning equipment, has been designed using the requirements of the APS programs as a guide, i.e., test durations, propellant flowrates and pressures, and environment. The Bay 7 facility has been built, partially activated and will be ready for the Igniter-Complete Thruster Tests at high chamber pressure. The Igniter-Complete Thruster Tests at low chamber pressure will be performed in the J Area Test Facility. A complete facility is currently being prepared in the J-3 altitude facility for these tests.

a.

II, B, Task II - Igniter Tests (cont.)

a. Aerophysics Laboratory

The majority of cold flow testing is being accomplished in this facility. The setup required consists of mounting the igniter configuration to be tested on an existing flow bench. Propellant supply lines are connected between the laboratory supply of the gases required and the test unit. The unit is then instrumented for the required temperatures and pressures, and the proper flow-control orifices are installed. The laboratory equipment is extremely flexible and capable of operation over wide ranges of flow, pressures and temperatures. Very little setup is required for the igniters, and virtually none is needed between series of tests.

b. Physics Laboratory

Two test positions have been setup in the Physics Laboratory. The first, Bay 1, will be used for the Igniter-Only Tests, and the second, Bay 7, will be used for Igniter-Complete Thruster Tests at high chamber pressure. Brief descriptions of the setup status for each location follow.

(1) Test Bay 1

Test Bay 1 of the Physics Laboratory was chosen for the Igniter-Only Tests because of the suitability of existing equipment. The capability of testing at altitude conditions using the propellant combination of gaseous oxygen and gaseous hydrogen is the primary function of Bay 1. In addition, the facility includes high pressure spheres that are currently capable of conditioning the pressurized, gaseous propellants down to liquid nitrogen temperature, and controlling their flows to a test apparatus.

II, B, Task II - Igniter Tests (cont.)

Setup of the new test position has been accomplished alongside the 3 ft dia vacuum duct located in front of and leading to Bay 1. A hole was cut in the duct and a 16 in. dia flange has been welded over the hole to provide access to the vacuum system for igniter firings. The propellant conditioning spheres have been moved to the new position, and a new cable tray containing the required instrumentation and process control cables has been installed between the bay and the new location. Supply lines for gaseous oxygen and gaseous hydrogen have been plumbed to the new position and the pressurization/bent "trees" were completed. The installation has been flowed with gaseous propellants, the electrical circuits have been checked, and the facility is ready for testing using propellants at ambient and below-ambient temperatures.

Buildup of the test hardware began with fabrication of an igniter mount and an integral high-vacuum fixture. The fixture is connected directly to the mount and is located within the vacuum duct. This combination forms a duct closure and a 4 in. dia x 6 in. long cylindrical volume into which the igniters will fire. The required hard vacuum will be established within the fixture and the overpressures will be received during firings by a spring loaded door that is part of the fixture. Subsequent to opening, the door will close automatically to permit re-establishment of the hard vacuum. Both the high and low P_c Igniter-Only Tests will be conducted in this facility.

(2) Test Bay 7

Because of the additional instrumentation, increased propellant requirement, and lack of physical space in Bay 1 for the Igniter-Complete Thruster Tests, a new test stand with ancilliary equipment has been built in Bay 7 for this program. The stand itself, the propellant conditioning

equipment, flow circuits and electrical controls are essentially complete, but require final activation. Work is continuing in Bay 7 and the facility is scheduled for completion during the coming program month. The Igniter-Complete Thruster and the Ignition Durability Tests for the high P_c design point will be conducted using this facility.

c. J-3 Test Facility

The following modifications were made to the J-3 test facility during this report period for the Igniter-Complete Thruster and Ignition Durability Tests for the low P_c design point: The design of the required modification was completed; material was procured for these modifications; the 2 in. propellant pressure valves and regulators were installed and actuation pressure was plumbed as required; the three flow control valves were installed with their hydraulic system; the thrust frame was modified and installed in the test cell; the Direct-Rite oscillograph (Model 5-123) was installed; the installation of control circuits for all remote operated valves was initiated; and the 6 in. venturis and flow spools were fabricated and calibrated.

3. Electrode Durability Tests

The purpose of the Electrode Durability Tests is to determine the suitability of various electrode materials for the spark and plasma plugs for extended duty cycle at igniter operating conditions.

a. Spark

The spark electrode durability tests were completed during this report period. One million discharge pulses were run on each

of the three candidate electrode materials, i.e., Inconel, nickel, and 347 stainless steel. All tests were conducted with an oxygen flow of 0.01 lb/sec through the plug at a pressure of 100 psia. Discharge energy was 10 millijoules. A planned fourth test of the stainless steel electrode at 5 millijoules was not conducted because of the satisfactory performance of this material at 10 millijoules.

(1) Test Setup

Figure 23 is a photograph of the test setup, which is also shown schematically in Figure 24. The setup consists of a system for metering oxygen and setting igniter back pressure, a spark power supply, sequencing controls, and instrumentation for monitoring and recording the test parameters. Oxygen flow rate and spark chamber pressure were monitored continuously on a digital data system and recorded periodically on an oscillograph. Spark pulse voltage and pulse time length were monitored continuously on an oscilloscope; the output of the oscilloscope was recorded periodically. Recording times were continuous from 1 to 10^4 pulses, and then for one-minute periods at 2×10^4, 5×10^4, 10^5, 2×10^5, 5×10^5 and 10^6 pulses. Both low and high speed records were made to check pulse train repeatability and to monitor pulse voltage. Figure 25 is a copy of a portion of the oscillograph record showing typical operation.

Nominal pulse rate was 500 pulses per second on for 75 millisec and off for 275 millisec. The GLA PN 30342 spark power source, commanded by an external control system, provided the spark pulses. Each pulse consisted of a high voltage (about 30KV) RF discharge, of durations too short to be seen on the oscillograph trace, followed by a lower voltage (4-5KV) DC discharge. Voltage across the plug gap was monitored directly in the first three tests. As no HV access ports were available in the power supply-cable-

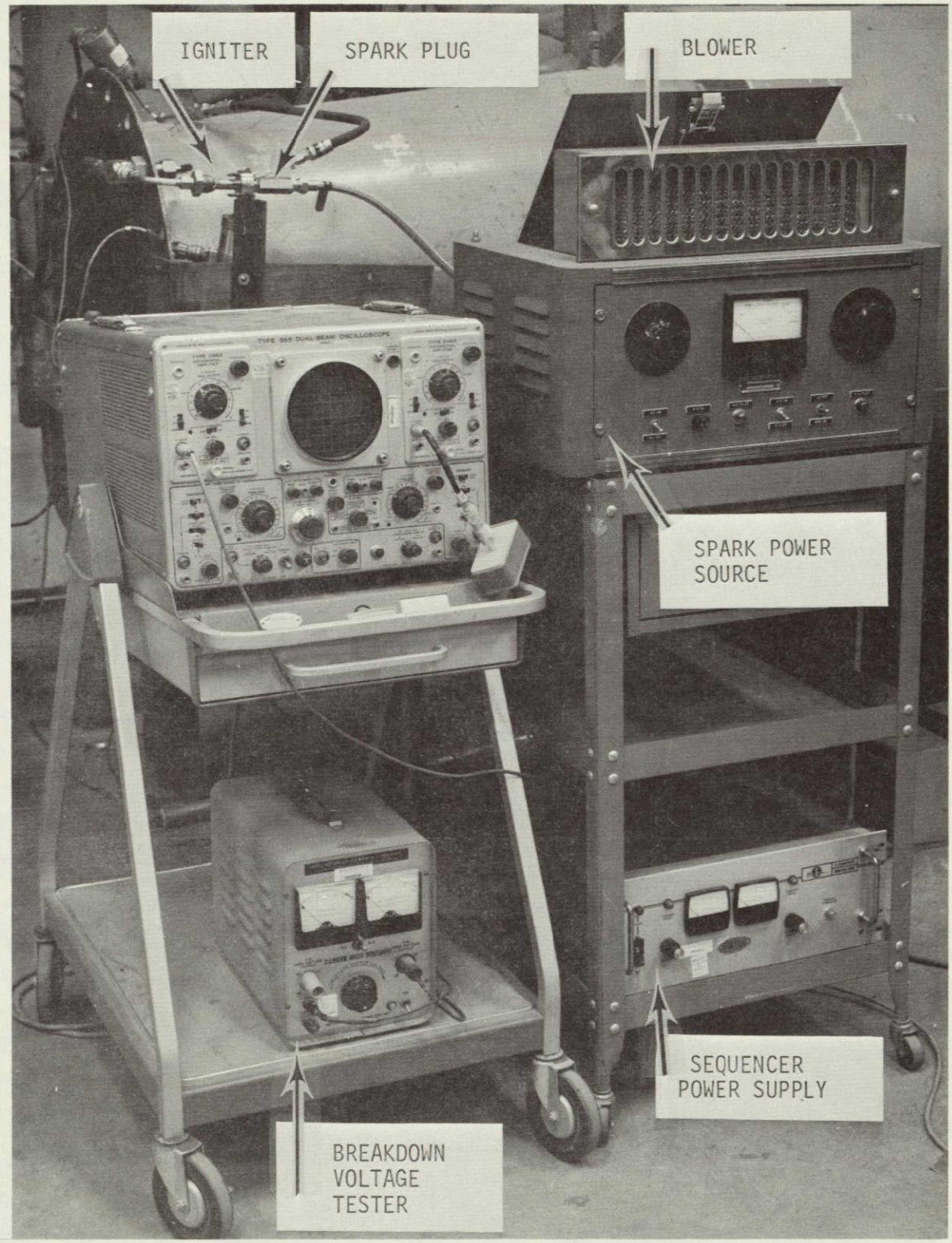

Figure 23. Spark Electrode Test Setup

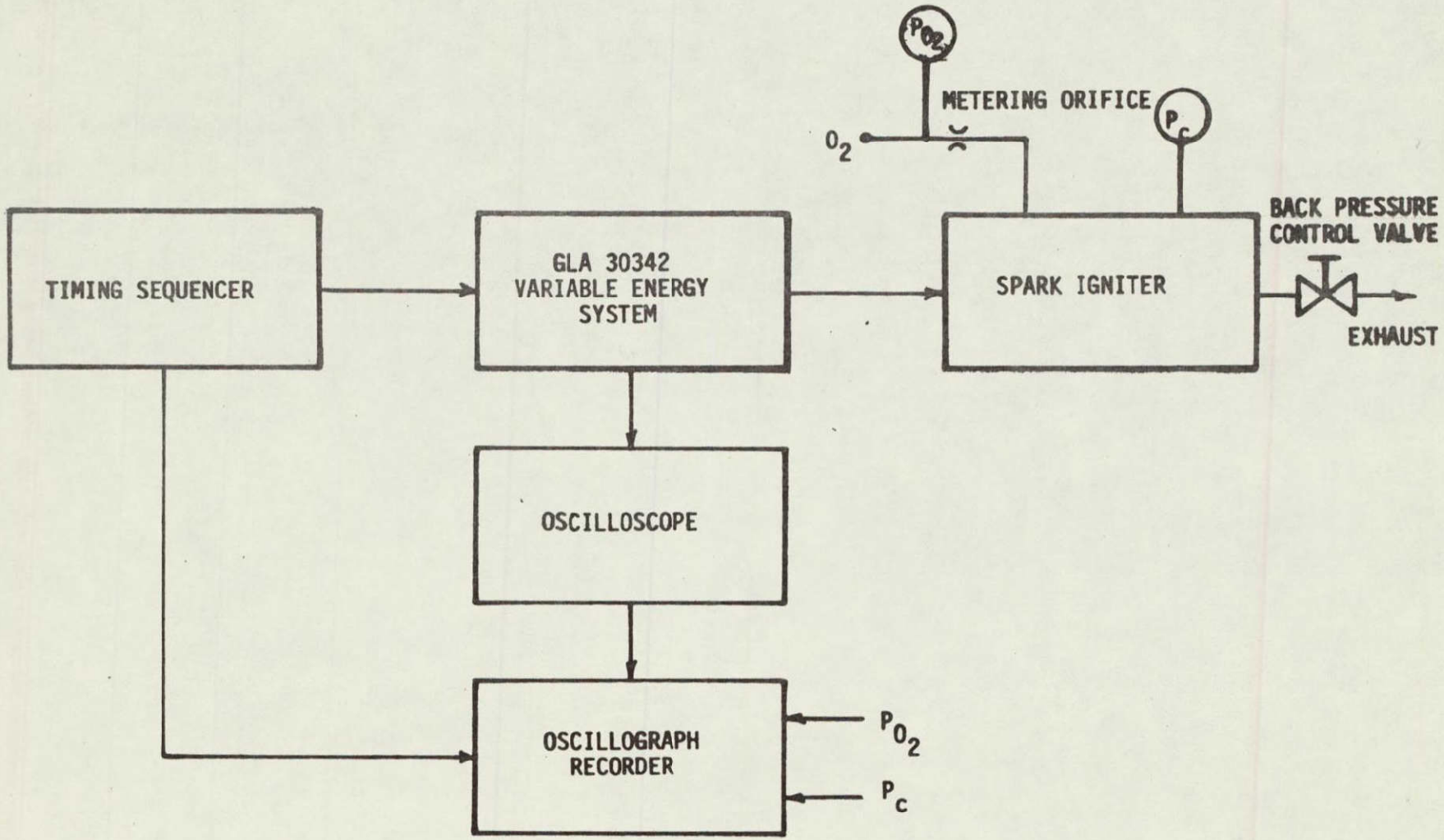

Figure 24. Spark Igniter Test Setup Schematic

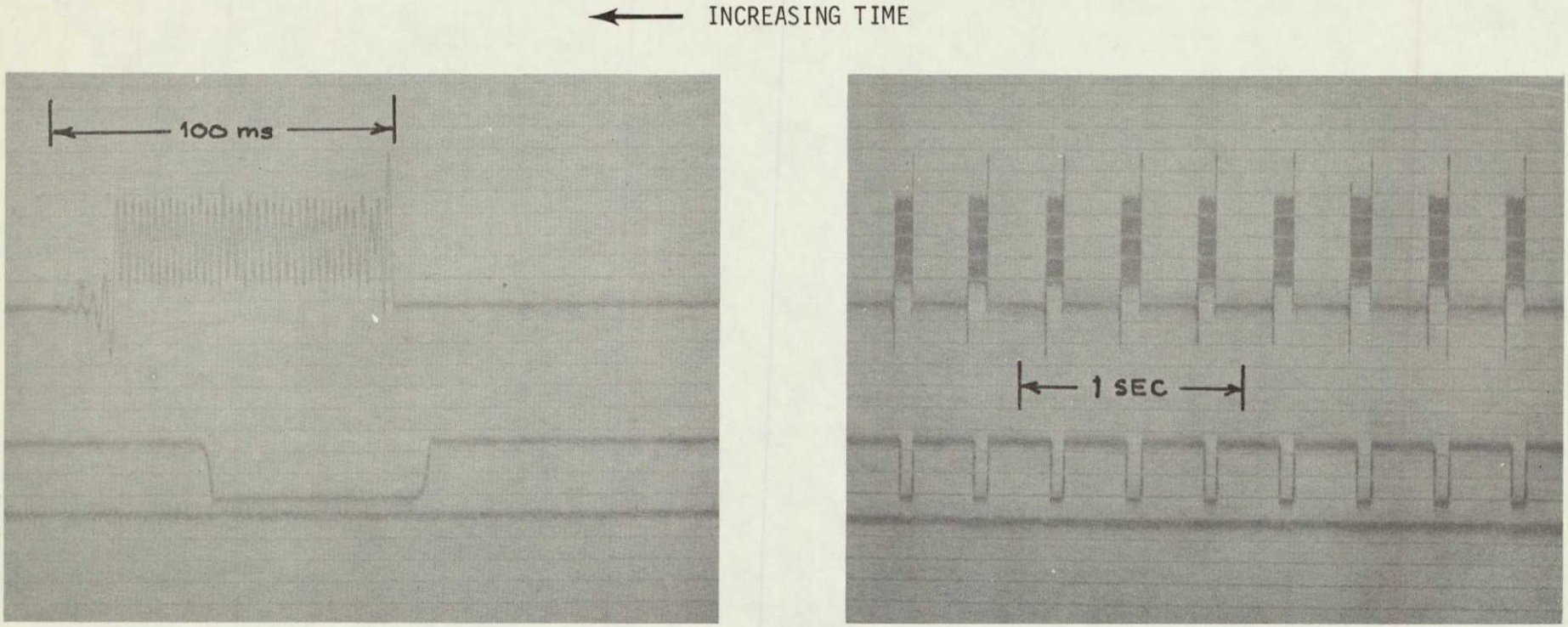

High Speed Record

Low Speed Record

Upper Trace: Spark gap voltage, 800 V/in.
Middle Trace: Command signal (negative step = ON signal)
Lower Trace: Reference
Horizontal Grid: 10 lines/in.

Figure 25. Typical Spark Pulse Train From Oscillograph Record

plug assembly, an adapter section was made to provide high voltage access at the connection between the power supply and the cable. The Teflon insulator in this adapter failed twice in attempts to test the first steel electrode. As a result, a pulse monitor output provided on the power supply was used for the last test. It gave a faithful reproduction of the pulse rate but indicated more variation in pulse-to-pulse voltage than was found in the direct voltage measurement.

(2) Test Results

The results of the tests are summarized in Table VI. Progressive change in breakdown voltage is shown in Figure 26. The results for each electrode material test are discussed below.

(a) Inconel

The appearance of this electrode before and after test is shown in Figures 27 and 28. Part way through the test, breakdown occurred at the ceramic insulator surface. Posttest examination showed breakdown only at the normal gap and not across the ceramic, indicating the abnormal breakdown occurred only intermittantly. The abnormal breakdown results in slightly reduced electrode erosion. However, as Inconel did not show outstanding performance when compared with the other electrode materials, it was not retested. The first three photos of Figure 29 show more detail of the Inconel electrode erosion. The abnormal breakdown was caused by an excessively long cathode insert which resulted in a narrow gap near the anode support and ceramic insulator. When the normal electrode gap opened slightly due to wear during the tests, the insulator surface gap was stressed too highly and broke down. This problem was eliminated in subsequent tests by boring out the inner section of the cathode insert to widen the gap in this area. No further insulator breakdown occurred.

TABLE VI

SUMMARY OF SPARK ELECTRODE DURABILITY TESTS

Run No.	Cathode Material	Anode Material	Test Medium	P_c Pressure (psia)	$\dot{w}$ (lb/sec)	Spark Energy (millijoule)	Cath. Wt. Pre-test (gm)	Cath. Wt. Post-test (gm)	Cath. Δ Wt. Loss (gm)	Anode Dia. Pre-test (in.)	Anode Dia. Post-test (in.)	Anode Δ Dia. Change (in.)	Gap Breakdown Voltage @ 1 atm, Air Pretest	Gap Breakdown Voltage @ 1 atm, Air Posttest	Comments
I-1	Inconel	Nickel	O_2	100	0.01	10	1.9401	1.9157	0.0244	0.193	0.181	0.012	4.4 KV	4.5 KV	Some discharge over surface of ceramic insulator.
N-1	Nickel	Nickel	O_2	100	0.01	10	1.0403	1.0284	0.0119	0.181	0.171	0.010	4.6 KV	5.2 KV	
S-1	347 S.S.	Nickel	O_2	100	0.01	10	1.0124	---	---	0.193	---	---	4.3 KV	---	Teflon high voltage connector brokedown early in test.
S-2	347 S.S.	Nickel	O_2	100	0.01	10	0.7935	0.7707	0.0228	0.193	0.177	0.016	4.5 KV	5.5 KV	

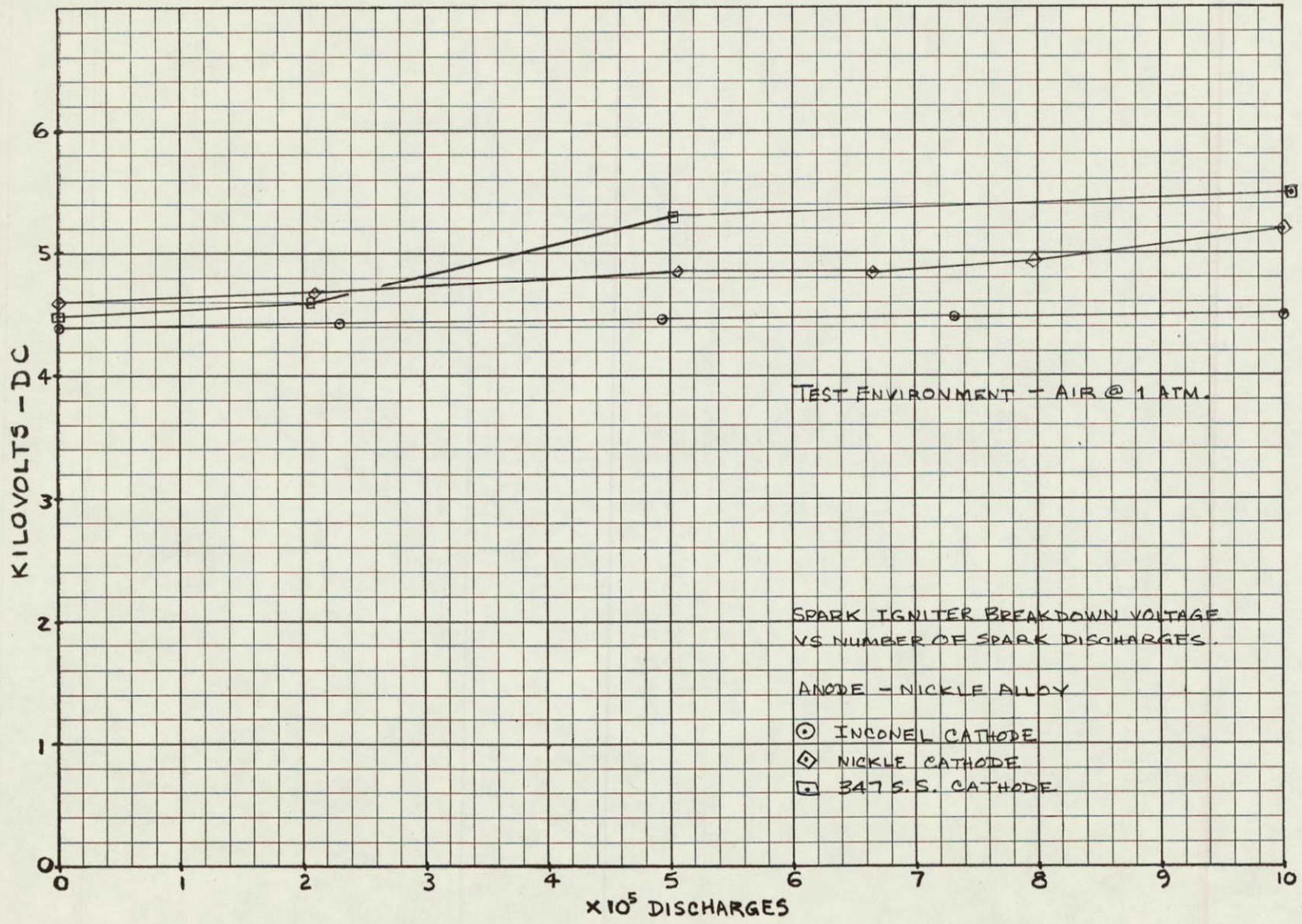

Figure 26. Spark Gap Breakdown Voltage as a Function of Pulse Life

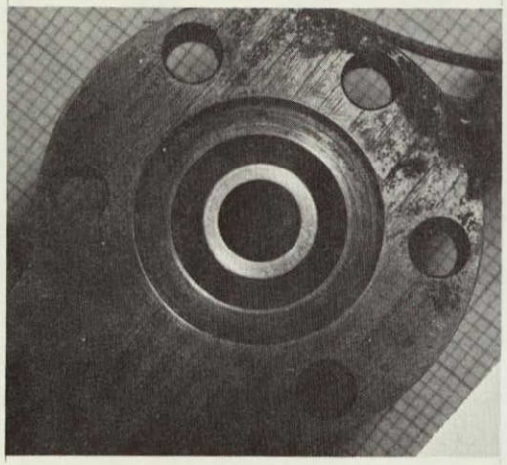

INCONEL CATHODE - PRE-TEST I-1

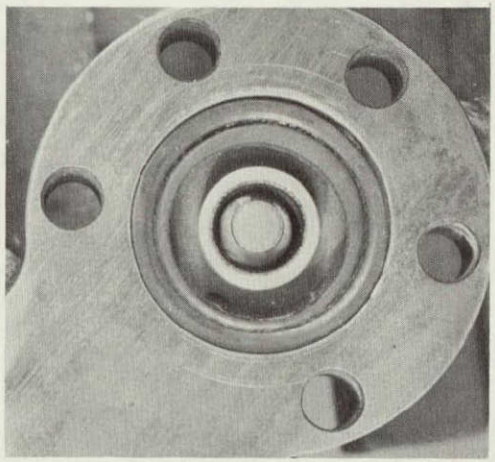

INCONEL CATHODE - POST-TEST I-1

1.4 x MAGNIFICATION

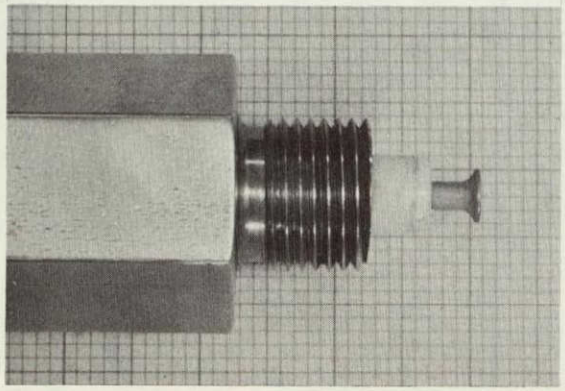

ANODE - INSULATOR ASSEMBLY
PRE-TEST I-1

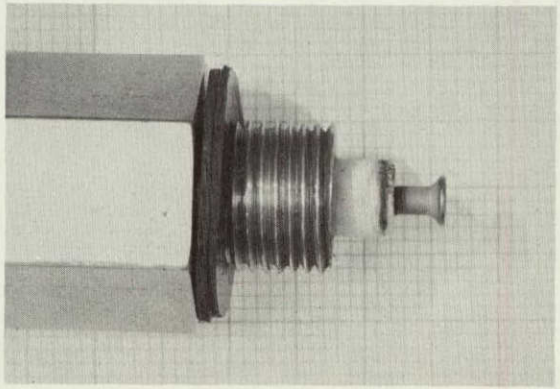

ANODE - INSULATOR ASSEMBLY
POST-TEST I-1

Figure 27. Inconel Electrode Before and After Test

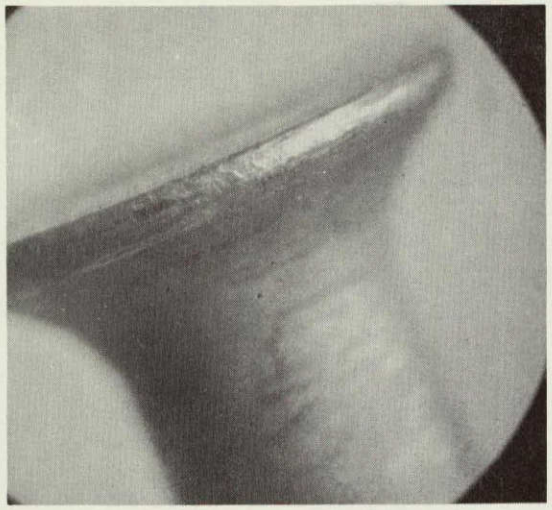

ANODE - PRE-TEST I-1 (15x)

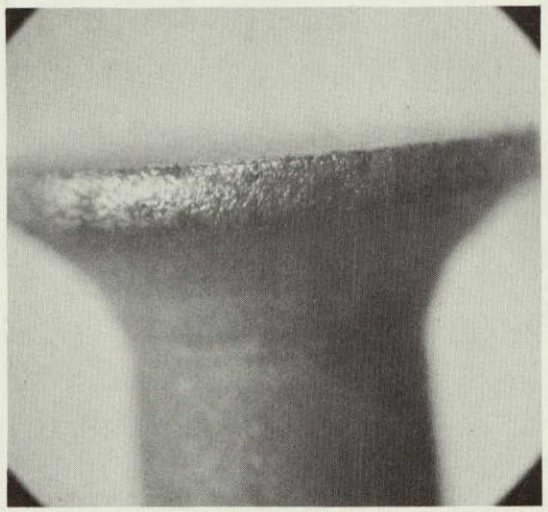

ANODE - POST-TEST I-1 (15x)

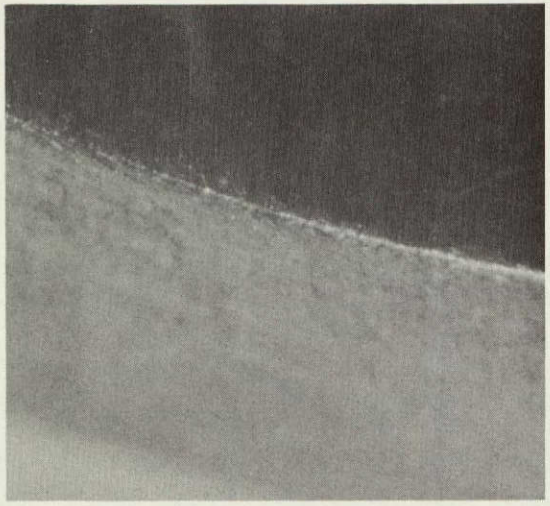

CATHODE DETAIL - PRE-TEST I-1
(30x)

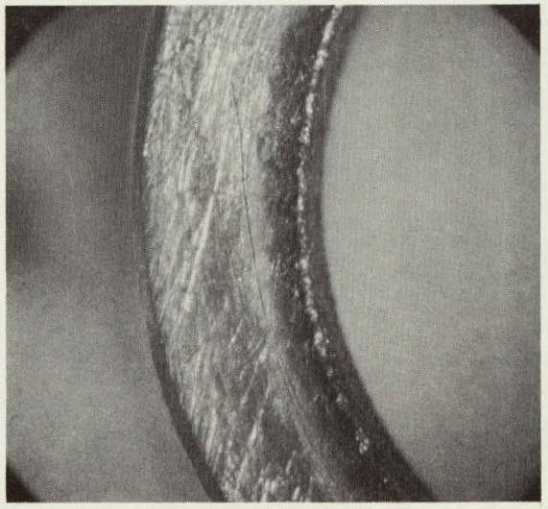

CATHODE DETAIL - POST-TEST I-1
(15x)

Figure 28. Details of Inconel Electrode Before and After Test

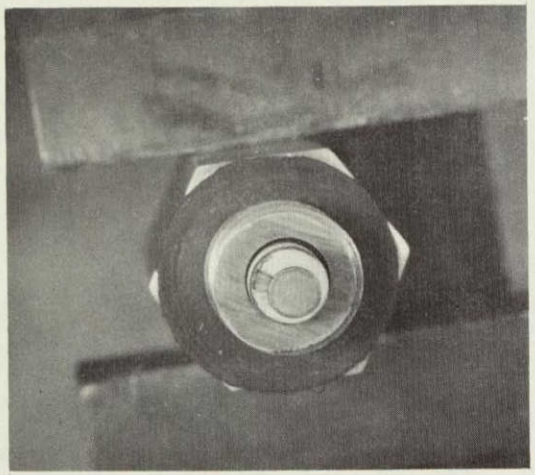

INSULATOR EROSION - POST-TEST I-1
(1.4x)

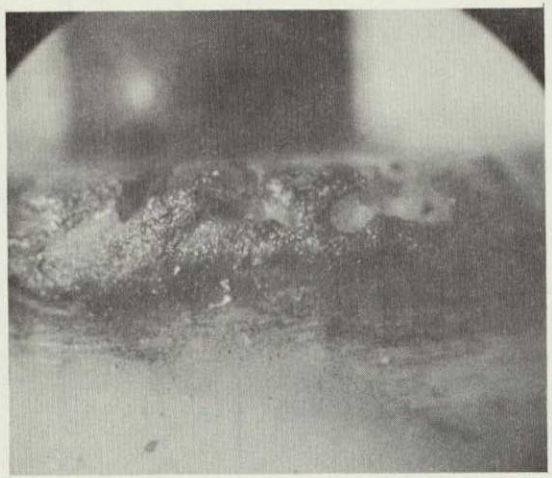

INSULATOR DETAIL - POST-TEST I-1
(15x)

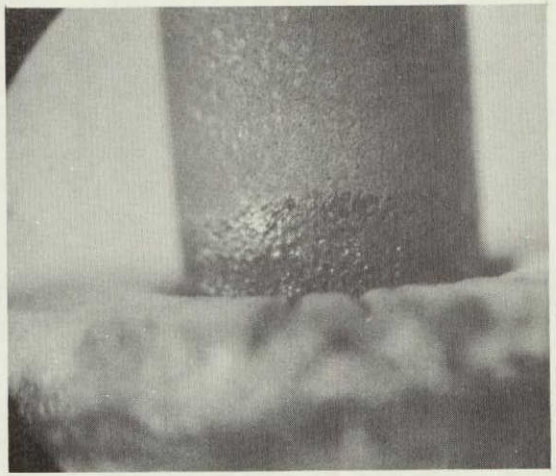

DETAIL OF INSULATOR DEPOSITS
POST-TEST I-1
(15x)

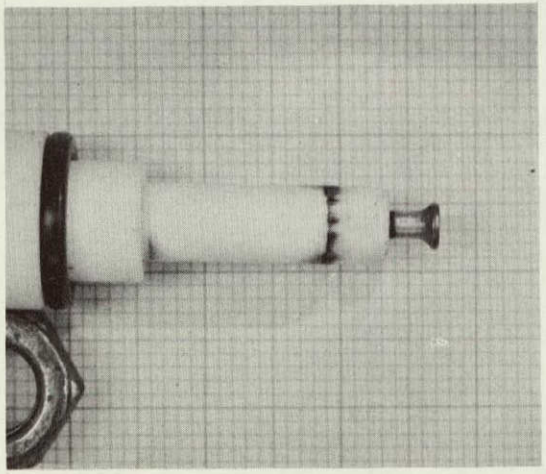

DEPOSITS ON INSULATOR
POST-TEST N-1
(1.4x)

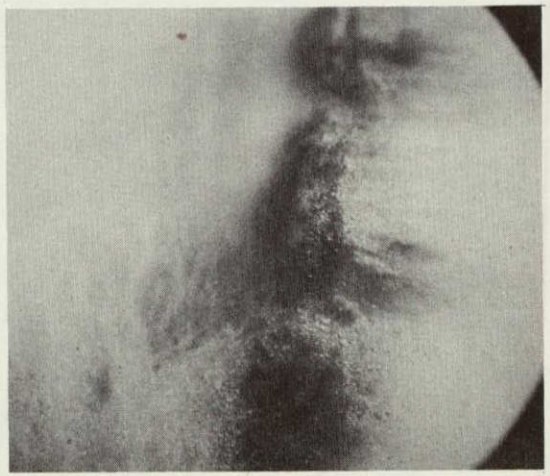

ELECTRODE SHAFT EROSION
POST-TEST I-1
(15x)

Figure 29. Details of Insulator Erosion and Sputter Deposits

(b) Nickel

The appearance of this electrode is shown before and after test in Figures 30 and 31. Performance is considered to be satisfactory with small, uniform wear and an air gap breakdown voltage increase from 4.6 KV at the start of testing to 5.2 KV at the end.

At the end of this test, dark deposits were noted on the insulator about 0.2 in. from the electrode end. These were initially believed to be the result of failure of the ceramic insulator. However, in breakdown tests up to 30 KV, no preferential discharge could be made to occur at these points. The deposits are shown in the last two photographs of Figure 29. Microscopic examination showed no cracks or pin holes. It is believed that capacitance coupling between the igniter case and center electrode of the RF trigger pulse caused gradual spittering of the case metal onto the insulator. A sharp corner in the case served to increase the field locally resulting in deposits which were very evident in 10^6 discharges. Other areas where sharp corners contacted the insulator were found to have slight stains, apparently due to the same cause. Although no spark plug failures resulted in these tests, the effect of capacitance-coupled sputtering should be considered in design of insulators for very long duty cycles.

(c) 347 Stainless Steel

The appearance of this electrode before and after a successful test is shown in Figures 32 and 33. It has an air gap breakdown voltage increase from 4.5 KV to 5.5 KV, slightly more than that for the nickel electrode. Its erosion based on weight loss was about twice that of the nickel electrode and a little less than that of the Inconel electrode. Erosion was uniform as before and sputtering deposits were apparent

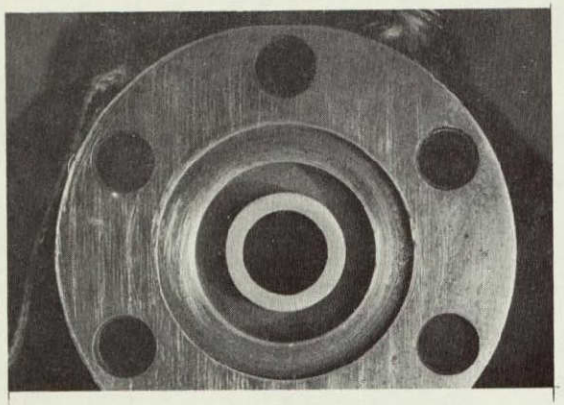

NICKEL CATHODE - PRE-TEST N-1

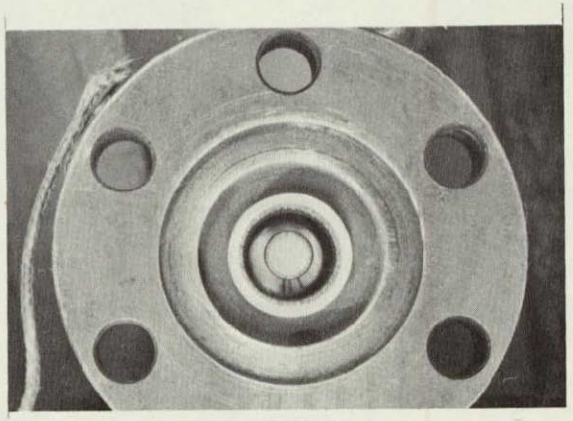

NICKEL CATHODE - POST-TEST N-1

1.4 x MAGNIFICATION

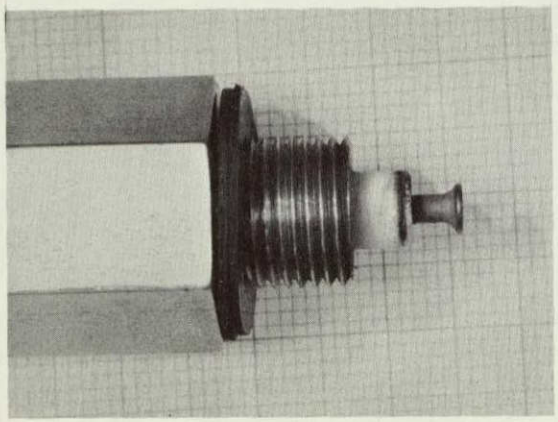

ANODE - INSULATOR ASSEMBLY
PRE-TEST N-1
(BEFORE CLEANING INSULATOR)

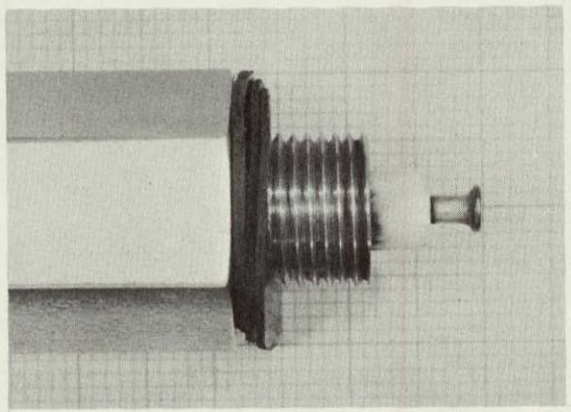

ANODE - INSULATOR ASSEMBLY
POST-TEST N-1

Figure 30. Nickel Electrode Before and After Test

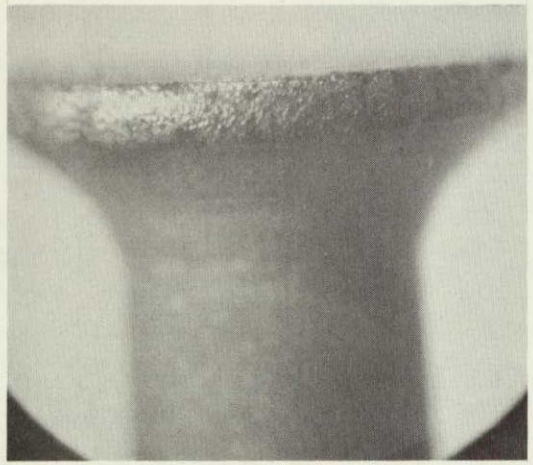

ANODE - PRE-TEST N-1

ANODE - POST-TEST N-1

15 x MAGNIFICATION

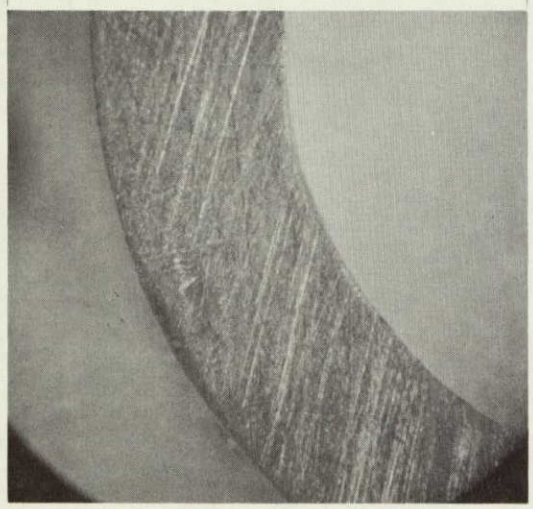

CATHODE - PRE-TEST N-1

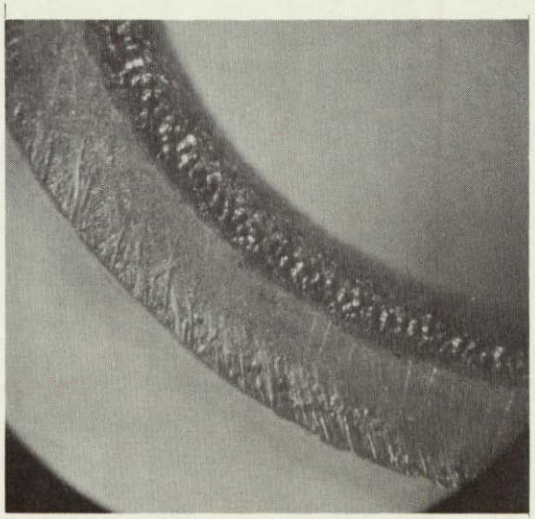

CATHODE - POST-TEST N-1

Figure 31. Details of Nickel Electrode Before and After Test

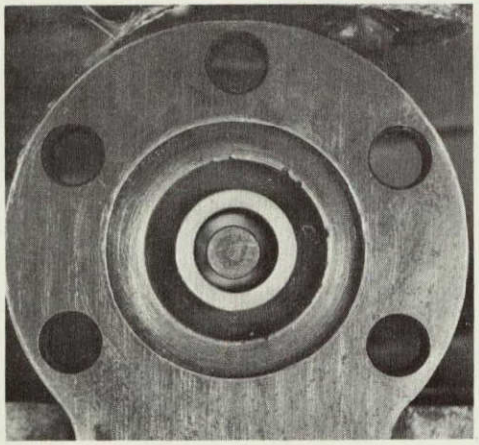

STAINLESS STEEL CATHODE
PRE-TEST S-2

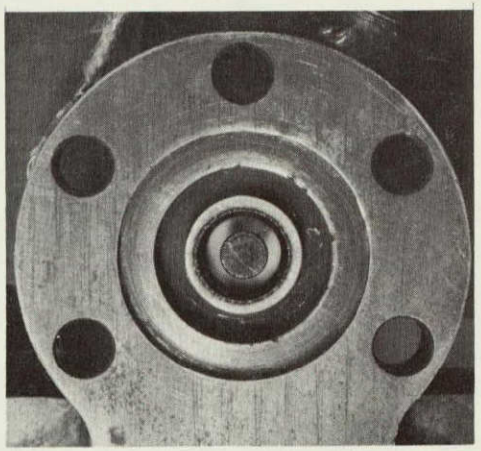

STAINLESS STEEL CATHODE
POST-TEST S-2

1.4 x MAGNIFICATION

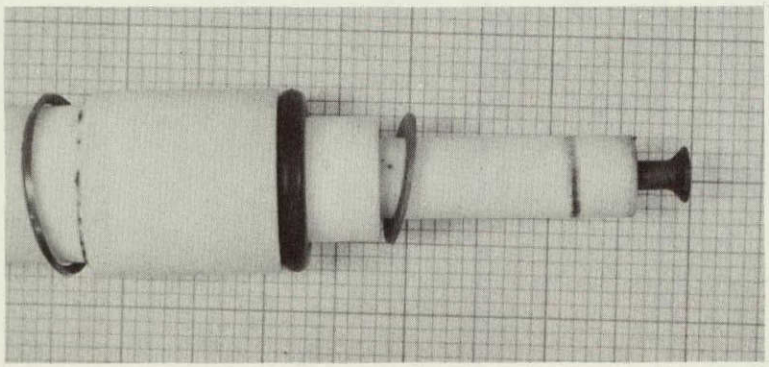

ANODE - INSULATOR ASSEMBLY
PRE-TEST S-2

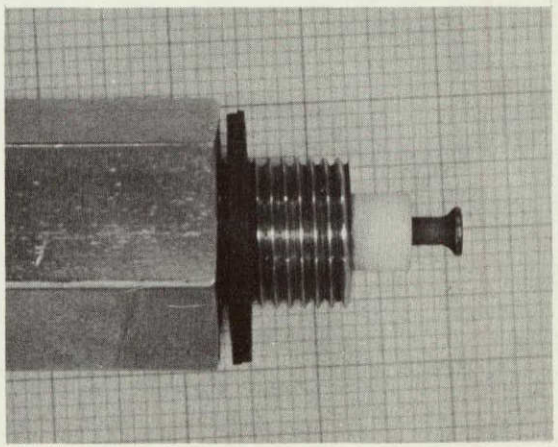

ANODE - INSULATOR ASSEMBLY
POST-TEST S-2

Figure 32. Stainless Steel Electrode Before and After Use

ANODE - PRE-TEST S-2

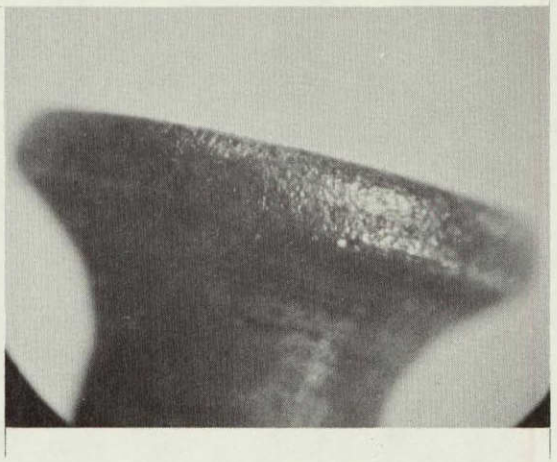

ANODE - POST-TEST S-2

15 x MAGNIFICATION

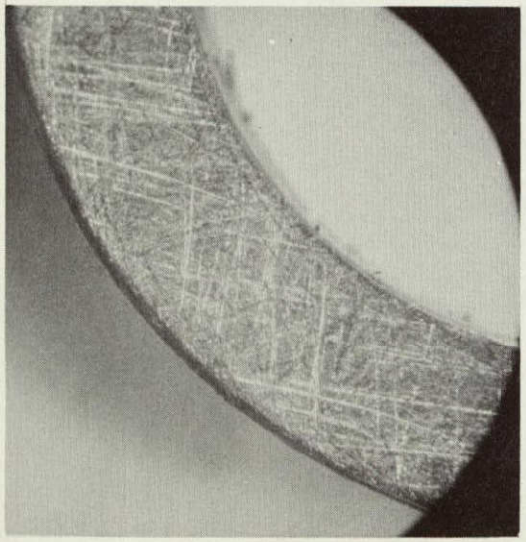

STAINLESS STEEL CATHODE
PRE-TEST S-2

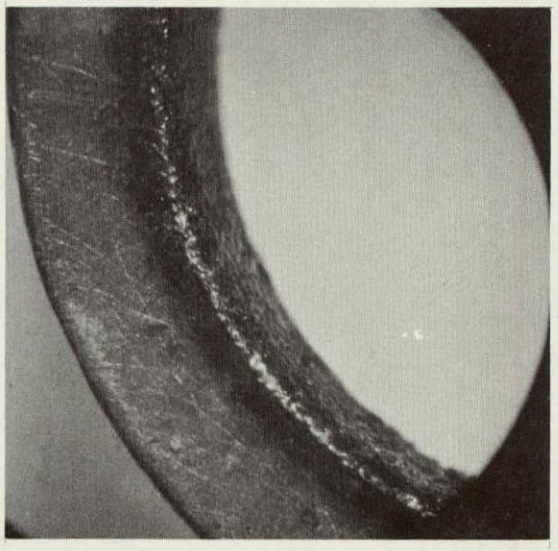

STAINLESS STEEL CATHODE
POST-TEST S-2

Figure 33. Details of Stainless Steel Electrode Before and After Test

on the insulator near the end of the case and at sharp corners on metal load rings, (Figure 29, photograph 3). DC breakdown of the insulator did not occur; the insulator successfully withstood a 30 KV breakdown test in air without arc through the insulator.

In the first attempt to test the steel electrode, an external high voltage connector failed. This failure apparently occurred very early in the test as no sign of discharge wear was noted on the electrode. A new connector was built and the test was resumed. This connector also failed. In neither case was a significant change noted in the monitored gap voltage, despite the drastic change in discharge conditions.

(3) Summary of Spark Electrode Durability Test Results

(a) Tentative relative ranking of materials in terms of least to worst erosion is nickel 1.0, stainless steel 1.9, Inconel greater than 2.1.

(b) All three materials eroded smoothly, with no catastrophic damage in 10^6 spark pulses, the equivalent of about 10^5 ignitions.

(c) The effects of RF discharges which can capacitance couple through the insulator must be considered in insulator design.

b. Plasma

A plasma plug was modified to accept screw-in inserts to permit testing with copper and stainless steel anodes. In addition, the high voltage plasma power supply was assembled, successfully tested by Crestronics and received at Aerojet. Figure 34 is a photograph of the power supply. Plasma electrode life tests have not yet begun.

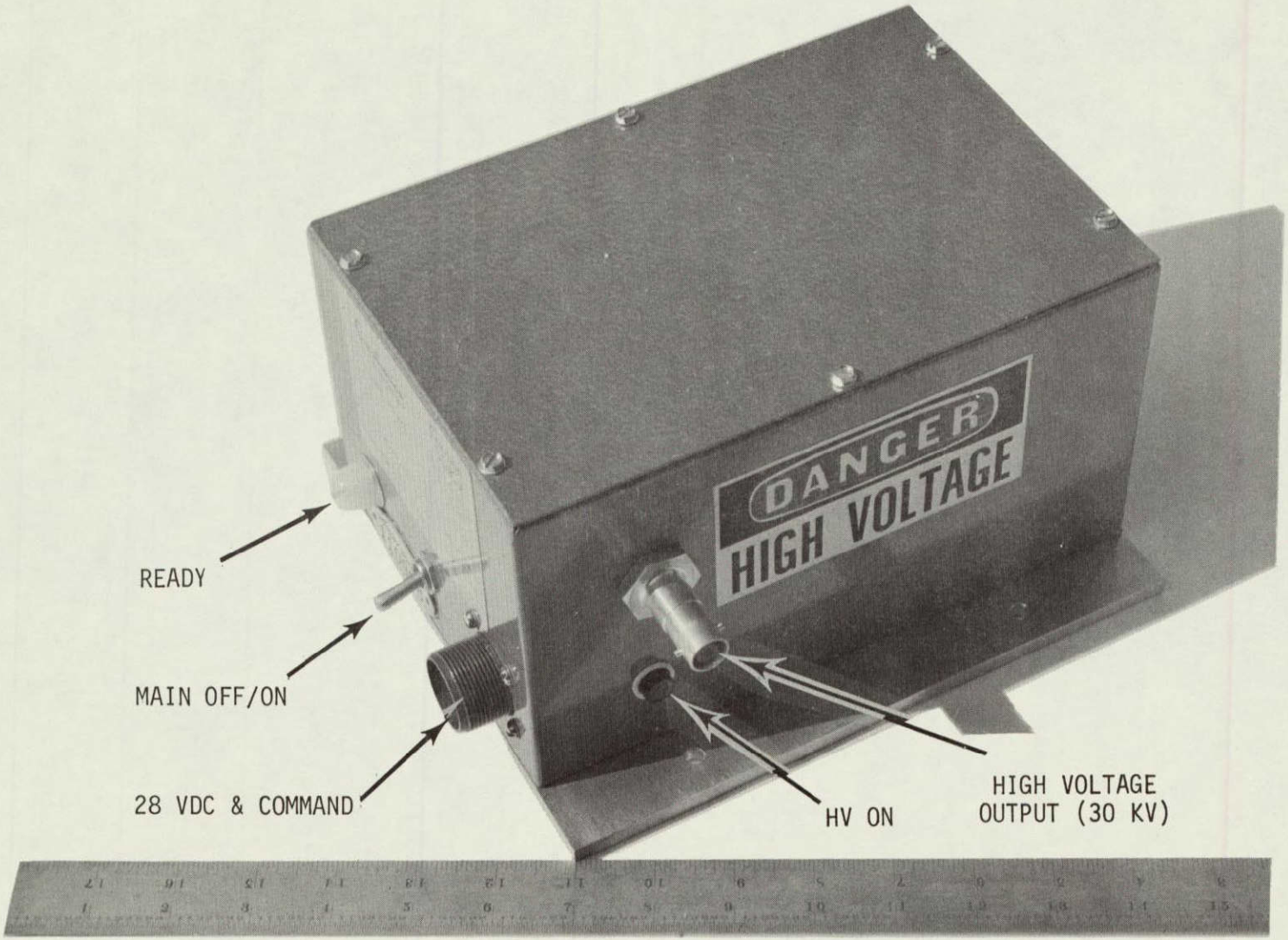

Figure 34. Plasma Igniter Power Supply

II, B, Task II - Igniter Tests (cont.)

4. Cold Flow Tests

a. Mixture Ratio Profile

The mixture ratio profile testing started near the end of this report period. The testing consists of simulating hydrogen and oxygen flow through the igniter with helium and nitrogen, and measuring their relative local concentrations, i.e., mixture ratio. To distinguish between the gases, the helium is heated to 200°F, while the nitrogen is cooled (by real gas effects during expansion) to a few degrees below ambient. Assuming turbulent mixing to be the primary energy transport mechanism, the gas temperature measured at any point corresponds to an unique mixture ratio. Normally, such tests have been conducted with hot helium and cold (-200°F) nitrogen to maximize the temperature difference and, therefore, the ΔT per point of mixture ratio change. However, near ambient nitrogen is used in these tests at high mixture ratio because the final mixed temperature is very close to the initial nitrogen temperature. This minimizes errors due to heat conduction into the system which would occur at cryogenic nitrogen temperatures.

The test setup for the mixture ratio tests is shown schematically in Figure 35. It consists of helium and nitrogen gas controls, and a helium heater. A single traversing thermocouple probe installed in the igniter chamber provides gas temperature distribution. The probe is mounted eccentrically so that it rotates through a large arc from side to side of the chamber and through its centerline. All but the last inch of the probe is supported against aerodynamic deflections by spring loading it against the chamber wall. The probe itself consists of a 2 mil chromel-alumel thermocouple in a 20 mil sheath. By rotating the probe mount about the chamber centerline, the probe can be traversed through any desired radial position.

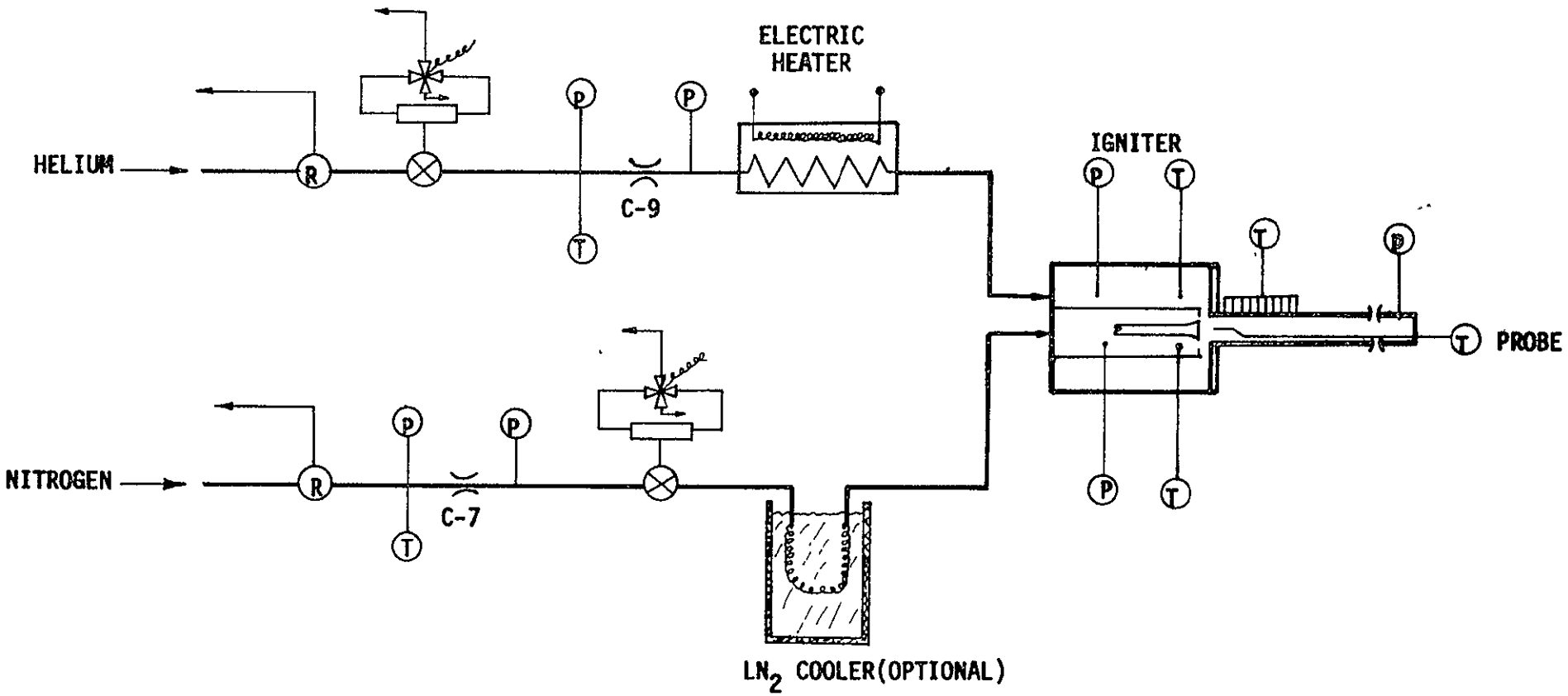

Figure 35. Schematic of Test Setup for Igniter Mixture Ratio Profile Test

In addition, the probe can be traversed longitudinally. To obtain mixture ratio at the wall, thin wall (0.020 in.) chamber is used, instrumented with eight thermocouples spot welded down its length.

The primary reason for conducting the mixture ratio survey tests is to determine the validity of the analytical predictions made for the spark and plasma pulse igniters. A generally fuel-rich zone was predicted along the wall of the spark igniter. If somewhat more mixing than predicted were to occur, a hot zone represented by transition from fuel rich through stoichiometric to oxidizer rich could result. On the other hand, the analysis for the plasma pulse igniter showed essentially unmixed oxygen on the chamber boundary. Unless more mixing occurs in actual test, this can represent a combustion problem if the outer hydrogen coolant flow fails to react with the outer, relatively cold oxygen of the core flow. The mixture ratio survey tests, therefore, have a direct bearing on igniter durability and performance.

b. Flow Calibration

Each igniter that will be used during the test program will be flow calibrated with either the actual gaseous propellant or a simulant, in which case the simulant flowrate will be corrected for specific heat ratio and molecular weight differences. The importance of adequate flow calibrations cannot be over-emphasized because these calibrations will control propellant flowrates which determine chamber pressure, mixture ratios and thrust level during tests. Adequate calibrations are an important protection against hardware damage.

Two calibrations are required before the igniters can be fired. The gaseous hydrogen "split" from the common fuel inlet must be

known to set the proper core mixture ratio. During calibration, the correct weight of fuel flow is metered to the hydrogen inlet by a critical flow venturi. The portion of fuel which flows to the core is captured at the throat with a special flow fixture that includes a back-pressure control valve and a flow measuring venturi. When the rate of hydrogen flow is known at the desired pressure settings, it is subtracted from the total inlet flow and the difference is the coolant flow. The "split" is then known. This calibration is performed at several conditions to give confidence in the data. From the total data, plots of weight flow versus pressure drop are prepared to select the proper values for tests. The oxygen circuit is flowed in similar fashion for calibration. However, no split is involved.

5. Additional Subtasks

Work has not started on the remainder of the Task II subtasks.

C. TASK III - IGNITION SYSTEM PRELIMINARY DESIGN

Work has not started on this task.

D. TASK IV - REPORTING REQUIREMENTS

The Work Plan and Test Plan for the program were submitted for review and approval. Written approval was received for each plan. The first and second Monthly Technical Progress Narratives were submitted.

III. CURRENT PROBLEMS

There are no current problems.

IV. FUTURE WORK

A. TASK I - IGNITER DESIGN AND FABRICATION

The fabrication of the spark and plasma pulse igniters for the low chamber pressure design point will be completed.

B. TASK II - IGNITER TESTS

1. Ignition Analysis

Work will continue with the Transient Flow and Turbulent Mixing and Combustion Computer Programs with the calculation of ignition limit curves.

2. Facility Setup in Bay 1

The setup of the Bay 1 facility to conduct the Igniter-Only Test Program will be completed.

3. Facility Setup in Bay 7

The setup of the Bay 7 facility to conduct the Igniter-Complete Thruster Test Program will be completed.

4. Facility Setup in J-3

The setup of the J-3 facility to conduct the Igniter-Only and Igniter-Complete Thruster Test Programs will continue.

IV, B, Task II - Igniter Tests (cont.)

5. Electrode Durability Tests

The plasma pulse electrode durability tests will be completed.

6. Cold Flow Calibration Tests

The Mixture Ratio Profile and Flow Calibration Test Programs will continue.

7. Igniter-Only Tests

The Igniter-Only Test Program will be initiated with the evaluation of the spark igniter.

8. Igniter-Complete Thruster Tests

The Igniter-Complete Thruster Test Program will be initiated with the evaluation of the spark igniter.

C. TASK IV - REPORTING REQUIREMENTS

Reports will be submitted as scheduled, see Figure 36.